

A priori bounds and global bifurcation results for frequency combs modeled by the Lugiato-Lefever equation

Rainer Mandel, Wolfgang Reichel

CRC Preprint 2016/7 (revised), October 2016

KARLSRUHE INSTITUTE OF TECHNOLOGY

CRC 1173



Participating universities



Universität Stuttgart

EBERHARD KARLS
UNIVERSITÄT
TÜBINGEN



Funded by

DFG

ISSN 2365-662X

A PRIORI BOUNDS AND GLOBAL BIFURCATION RESULTS FOR FREQUENCY COMBS MODELED BY THE LUGIATO-LEFEVER EQUATION

RAINER MANDEL AND WOLFGANG REICHEL

ABSTRACT. In nonlinear optics 2π -periodic solutions $a \in C^2([0, 2\pi]; \mathbb{C})$ of the stationary Lugiato-Lefever equation $-da'' = (i - \zeta)a + |a|^2a$ – if serve as a model for frequency combs, which are optical signals consisting of a superposition of modes with equally spaced frequencies. We prove that nontrivial frequency combs can only be observed for special ranges of values of the forcing and detuning parameters f and ζ , as it has been previously documented in experiments and numerical simulations. E.g., if the detuning parameter ζ is too large then nontrivial frequency combs do not exist, cf. Theorem 2. Additionally, we show that for large ranges of parameter values nontrivial frequency combs may be found on continua which bifurcate from curves of trivial frequency combs. Our results rely on the proof of a priori bounds for the stationary Lugiato-Lefever equation as well as a detailed rigorous bifurcation analysis based on the bifurcation theorems of Crandall-Rabinowitz and Rabinowitz. We use the software packages AUTO and MATLAB to illustrate our results by numerical computations of bifurcation diagrams and of selected solutions.

1. INTRODUCTION

In physics literature an optical signal is called a frequency comb if it consists of a superposition of modes with equally spaced frequencies. By a suitable choice of reference frame a frequency comb becomes stationary (time-independent). For $k \in \mathbb{Z}$ let \hat{a}_k denote the complex amplitude of the k -th mode of the signal in the frequency domain and let $a(x) = \sum_{k \in \mathbb{Z}} \hat{a}_k e^{ikx}$ be the associated Fourier series. A commonly used mathematical model is given by the stationary Lugiato-Lefever equation

$$(1.1) \quad \begin{aligned} -da_1'' &= -a_2 - \zeta a_1 + (a_1^2 + a_2^2)a_1, \\ -da_2'' &= a_1 - \zeta a_2 + (a_1^2 + a_2^2)a_2 - f, \\ a_1, a_2 & \text{ } 2\pi\text{-periodic} \end{aligned}$$

where the parameters satisfy $d \neq 0$ and $\zeta, f \in \mathbb{R}$ and $a(x, t) = a_1(x) + ia_2(x)$, i.e., a is split into its real and imaginary part. Derivations of (1.1) may be found, e.g., in [2, 12]. More details on the physical background and the meaning of the parameters are given in Section 1.2. Equation (1.1) is a nonvariational version of the stationary nonlinear Schrödinger equation

Date: October 31, 2016.

2000 Mathematics Subject Classification. Primary: 34C23, 34B15; Secondary: 35Q55, 35Q60.

Key words and phrases. nonlinear Schrödinger equation, frequency combs, damping, forcing, bifurcation, Lugiato-Lefever equation.

with added damping and forcing. Our analysis and our results are based on the investigation of (1.1) from the point of view of bifurcation from trivial (i.e. spatially constant) solutions.

1.1. Mathematical context and main results. One first notices that (1.1) has trivial, i.e. spatially constant, solutions. They correspond to vanishing amplitudes of all modes except the 0-mode and are described in detail in Lemma 6 below. Stable, spatially periodic patterns bifurcating from trivial solutions of (1.1) were already observed in [19]. Recently, a more far-reaching bifurcation analysis appeared in [9] (see also [8] for a detailed mathematical analysis) where the differential equation in (1.1) is considered as a four-dimensional dynamical system in the unknowns a_1, a'_1, a_2, a'_2 . As the parameters f and ζ change, the trivial solutions exhibit various bifurcation phenomena. This approach allows an extensive account of various possible types of solutions of the differential equations in (1.1). However, with this approach the 2π -periodicity of the solutions may be lost. An emanating solution with spatial period τ has to be rescaled to the fixed period 2π and as a result (1.1) is changed, e.g., d becomes $(2\pi)^2 d/\tau^2$. A different view on bifurcation has been developed in [20]. Here spatially 2π -periodic solutions of (1.1) are considered via a bifurcation approach using the center manifold reduction. The resulting picture is very detailed in the vicinity of special parameter values but beyond these values nothing seems to be known – a gap in the literature which we would like to fill with the present paper.

Similarly to the above-mentioned papers we use bifurcation theory to prove the existence of frequency combs bifurcating from the set of spatially constant solutions. Let us therefore point out the main features which distinguish our approach from the previous ones. Unlike [8, 9] we consider (1.1) on certain spaces of 2π -periodic functions. We obtain a very rich bifurcation picture which is not limited to local considerations as in [8, 9, 20]. In Theorem 1 and Theorem 2 we find a priori bounds and uniqueness results which allow us to show that

- (a) nonconstant solutions of (1.1) only occur in the range $\text{sign}(d)\zeta \in [\zeta_*, \zeta^*]$,
- (b) nonconstant solutions of (1.1) satisfy $\|a\|_\infty + |\zeta| \leq C$.

Here, the values ζ_*, ζ^* and C are explicit and only depend on the parameters f, d . We begin with our results concerning pointwise a priori bounds for solutions of (1.1) in terms of the parameters ζ, d, f .

Theorem 1. *Let $d \neq 0, f, \zeta \in \mathbb{R}$. Every solution $a \in C^2([0, 2\pi], \mathbb{R}^2)$ of (1.1) satisfies*

$$(1.2) \quad \|a\|_{L^\infty} \leq \frac{|f|(1 + 12\pi^2 f^2 |d|^{-1})}{\max\{1, -\zeta \text{sign}(d) - \gamma(d, f)\}},$$

where

$$(1.3) \quad \gamma(d, f) := \begin{cases} 36\pi^2 f^4 |d|^{-1}, & d > 0, \\ 36\pi^2 f^4 |d|^{-1} + f^2(1 + 12\pi^2 f^2 |d|^{-1})^2, & d < 0. \end{cases}$$

Remark. Further bounds in $L^2([0, 2\pi], \mathbb{R}^2)$ and $H^1([0, 2\pi], \mathbb{R}^2)$ may be extracted from the proof of this theorem.

In our second result we employ Theorem 1 to show that the set of nonconstant solutions is bounded with respect to ζ .

Theorem 2. Let $d \neq 0, f \in \mathbb{R}, \zeta \in \mathbb{R}$ and let ζ_*, ζ^* be given by

$$\begin{aligned}\zeta_* &:= -\gamma(d, f) - \sqrt{6}|f|(1 + 12\pi^2 f^2 |d|^{-1}), \\ \zeta^* &:= 6f^2(1 + 12\pi^2 f^2 |d|^{-1})^2.\end{aligned}$$

Then every solution of (1.1) is constant provided $\text{sign}(d)\zeta < \zeta_*$ or $\text{sign}(d)\zeta > \zeta^*$.

Next we consider (1.1) from the point of view of bifurcation theory where one of the two values f or ζ is fixed and the other one is the bifurcation parameter. According to the two possible choices we identify two curves of constant solutions: $\hat{\Gamma}_f$ with f being fixed and $\bar{\Gamma}_\zeta$ with ζ fixed, see Lemma 6 for explicit parametrizations of these curves. We investigate branches of nontrivial solutions that bifurcate from the trivial branches $\hat{\Gamma}_f$ and $\bar{\Gamma}_\zeta$ and obtain information about their global shape. In our approach we consider the following special class of solutions of (1.1). We call them synchronized solutions in order to emphasize that they have a particular shape.

Definition 3. A 2π -periodic solution $a \in C^2([0, 2\pi]; \mathbb{C})$ of (1.1) is called synchronized if $a'(0) = a'(\pi) = 0$.

Remarks. (a) Synchronized solutions are even around $x = 0$ and $x = \pi$. The advantage of considering synchronized solutions is that the translation invariance of the original equation (1.1) is no longer present in this Neumann boundary value problem which makes the bifurcation analysis much easier, see also the remark after Proposition 11.

(b) It would be interesting to find out whether (1.1) admits solutions which are not synchronized. Note that in the case of scalar periodic boundary value problems the restriction to homogeneous Neumann boundary conditions on an interval of half the period is natural since (up to a shift) all solutions satisfy this condition. However, in the system case this is not clear at all and we have to leave it as an open problem.

Before we state our results let us recall some common notions in bifurcation theory. In the context of bifurcation from $\hat{\Gamma}_f$ (Theorem 4) a pair (a, ζ) is called a trivial solution if it is spatially constant, i.e., if (a, ζ) lies on $\hat{\Gamma}_f$. A trivial solution (a, ζ) is called a bifurcation point if a sequence $(a_k, \zeta_k)_{k \in \mathbb{N}}$ of non-trivial solutions of the periodic system (1.1) converges to (a, ζ) . Similarly trivial solutions and bifurcation points are defined when bifurcation from $\bar{\Gamma}_\zeta$ is investigated, see Theorem 5. Since our analysis of synchronized solutions is based on the bifurcation theorem of Crandall-Rabinowitz [4] such bifurcating non-trivial solutions lie on local curves around the bifurcation points. Furthermore, we will use the global bifurcation theorem of Rabinowitz [22] to show that these curves are part of a connected set that is unbounded or returns to the curve of trivial solutions at some other point. A continuum satisfying one of these two properties will be called global continuum. If, additionally, the nontrivial (i.e. nonconstant) solutions from this continuum are confined in a bounded subset of $L^\infty([0, 2\pi], \mathbb{R}^2) \times \mathbb{R}$ then the continuum will be called bounded.

For fixed $f \in \mathbb{R}$ we find that at most finitely many global continua bifurcate from $\hat{\Gamma}_f$. These continua are bounded and intersect $\hat{\Gamma}_f$ at another trivial solution. For the reader's convenience this is illustrated in the plots of Figures 7–14. The result reads as follows.

Theorem 4. *Let $d \neq 0, f \in \mathbb{R}$. If $|f| < 1$ then the curve $\hat{\Gamma}_f$ (see Lemma 6 (a)) does not contain any bifurcation point for (1.1). In case $|f| \geq 1$ the following holds:*

- (i) *All bifurcation points are among the points $(\hat{a}_1(t), \hat{a}_2(t), \hat{\zeta}(t))$ where the number $t \in [-\sqrt{1 - |f|^{-2}}, +\sqrt{1 - |f|^{-2}}]$ satisfies*

$$(1.4) \quad dk^2 = f^2(1 - t^2) - \frac{t}{\sqrt{1 - t^2}} - \sigma \sqrt{f^4(1 - t^2)^2 - 1}$$

for some $k \in \mathbb{N}$ and some $\sigma \in \{-1, 1\}$.

- (ii) *The curve $\hat{\Gamma}_f$ contains at most $\hat{k}(f)$ bifurcation points for (1.1) where*

$$\hat{k}(f) := 2(|d|^{-1}(f^2 + \sqrt{f^2 - 1} + \sqrt{f^4 - 1}))^{1/2}.$$

- (iii) *If in addition to (1.4) one has*

$$(S) \quad -k^2 + 2d^{-1}(f^2(1 - t^2) - t(1 - t^2)^{-1/2}) \neq j^2 \text{ for all } j \in \mathbb{N}_0 \setminus \{k\},$$

$$(T) \quad 4f^6t^3(1 - t^2)^2 + f^4(1 - t^2)^{1/2} - 2tf^2 - (1 - t^2)^{-3/2}$$

$$- \sigma \sqrt{f^4(1 - t^2)^2 - 1} \left(4f^4t^3(1 - t^2) + f^2(2t^2 - 1)(1 - t^2)^{-1/2} \right) \neq 0$$

then a global continuum containing nontrivial synchronized solutions emanates from $(\hat{a}_1(t), \hat{a}_2(t), \hat{\zeta}(t))$. This continuum is bounded and it returns to $\hat{\Gamma}_f$ at some other point. In a neighbourhood of $(\hat{a}_1(t), \hat{a}_2(t), \hat{\zeta}(t))$ the continuum is a curve consisting of $\frac{2\pi}{k}$ -periodic nontrivial synchronized solutions.

Remarks. The numbers k and t in (1.4) have the following meaning: if (1.1) is linearized at $(\hat{a}_1(t), \hat{a}_2(t), \hat{\zeta}(t))$ then $\alpha^k \cos(kx)$ with $\alpha^k \in \mathbb{R}^2 \setminus \{(0, 0)\}$ solves this linearized equation. From this fact we can draw several conclusion that are worth to be mentioned. The following remarks (a)-(d) are equally valid in the context of Theorem 5.

(a) Whenever t_0 is a turning point of the curve of trivial solutions, i.e. $\hat{\zeta}'(t_0) = 0$, then (1.4) is satisfied for $k = 0$. Since in this case typically (S) and (T) also hold a bifurcation from turning points $\hat{\Gamma}_f$ is predicted which, however, is not visible in any bifurcation diagram. The fact that this is not a contradiction to the Crandall-Rabinowitz Theorem is explained in detail at the beginning of Section 4.2.

(b) The integer k also represents the number of maxima of the bifurcating solutions close to the bifurcation point. In accordance with our numerical experiments this leads to the rule of thumb that k -solitons may be found on branches indexed with k . As mentioned in (a), at turning points of the curve of trivial solutions (1.4) is satisfied for $k = 0$ and some t_0 . Therefore, if $|d|$ is small enough, then (1.4) typically admits a solution for $k = 1$ and some t_1 near t_0 . Therefore, bifurcating branches with 1-solitons typically emanate near turning points of the curve of trivial solutions. Our numerical experiments in Section 5 confirm this.

(c) Suppose we have a bifurcation point corresponding to some numbers k, t . If we consider (1.1) as an equation in the space of $2\pi/k$ -periodic synchronized solutions then the Crandall-Rabinowitz Theorem shows the existence of a bifurcating branch consisting entirely of $2\pi/k$ -periodic synchronized solutions. This branch returns to the trivial curve at bifurcation points associated to multiples of k . A typical example can be found in the left bifurcation diagram of Figure 5 in Section 5.2. Within the broader space of synchronized solutions the branches consisting of $2\pi/k$ -periodic solutions persist but additional connections to the trivial branches can exist as the right bifurcation diagram in Figure 5 shows.

Another consequence of this observation can be seen in Figure 8 in Section 5.3 for the parameter values $f = 1.6, d = 0.1$. The theorem predicts bifurcation points precisely for $k \in \{1, 2, 3, 4, 5, 6, 7\}$, see Figure 7. For $k \in \{4, 5, 6, 7\}$ any integer multiple is larger than 7. Therefore continua emanating from the bifurcation points associated to $k \in \{4, 5, 6, 7\}$ have to return to the trivial branch at bifurcation points associated with the same k . This corresponds to the green, red, blue and pink branches in Figure 8.

(d) The bifurcation point divides the bifurcating curve from (iii) into two pieces. Each solution on one piece corresponds to a solution on the other via a phase shift by π/k . In other words two such solutions a, \tilde{a} are related by $\tilde{a}(x) = a(x + \pi/k)$. Since their L^2 -norms coincide the AUTO plots in Section 5 only show one curve near every bifurcation point. Accordingly, each point on this curve represents two solutions with the same L^2 -norm.

Now let us state the corresponding result for the bifurcation analysis associated to the family of trivial solutions $\bar{\Gamma}_\zeta$ for given $\zeta \in \mathbb{R}$. In contrast to the above results we find that infinitely many global continua emanate from $\bar{\Gamma}_\zeta$ in the case $d > 0$ whereas for $d < 0$ again only finitely many such continua can exist. The numerical plots from Figures 1–6 illustrate our results. Although we do not have a proof for the boundedness of the continua in this case, it seems nevertheless plausible in view of the numerical plots.

Theorem 5. *Let $d \neq 0, \zeta \in \mathbb{R}$.*

- (i) *All bifurcation points on the curve $\bar{\Gamma}_\zeta$ (see Lemma 6 (b)) are among the points $(\bar{a}_1(s), \bar{a}_2(s), \bar{f}(s))$ where*

$$(1.5) \quad |s| = \left(\frac{2}{3}(\zeta + dk^2) - \frac{\sigma}{3}\sqrt{(\zeta + dk^2)^2 - 3} \right)^{1/2}$$

for some $k \in \mathbb{N}, \sigma \in \{-1, 1\}$ and provided $\zeta + dk^2 \geq \sqrt{3}$.

- (ii) *If $d < 0$ then the curve $\bar{\Gamma}_\zeta$ contains at most $\bar{k}(\zeta)$ bifurcation points for (1.1) where*

$$\bar{k}(\zeta) := 4(|d|^{-1}(\zeta - \sqrt{3})_+)^{1/2}.$$

- (iii) *If in addition to (1.5) one has*

$$(S) \quad -k^2 + \frac{2}{3}d^{-1}(\zeta + 4dk^2 - 2\sigma\sqrt{(\zeta + dk^2)^2 - 3}) \neq j^2 \quad \text{for all } j \in \mathbb{N}_0 \setminus \{k\},$$

$$(T) \quad \zeta + dk^2 \neq \sqrt{3} \quad \text{and} \quad 4\zeta + dk^2 - 2\sigma\sqrt{(\zeta + dk^2)^2 - 3} \neq 0 \quad \text{and} \\ 2\zeta + 5dk^2 - 4\sigma\sqrt{(\zeta + dk^2)^2 - 3} \neq 0$$

then a global continuum containing synchronized and $\frac{2\pi}{k}$ -periodic nontrivial solutions bifurcates from $(\bar{a}_1(s), \bar{a}_2(s), \bar{f}(s))$. In a neighbourhood of this point the continuum is a curve consisting of $\frac{2\pi}{k}$ -periodic nontrivial synchronized solutions.

Remarks. (a) We may restrict our attention to the bifurcations occurring for positive f . Indeed, by Theorem 1 we have that for $f = 0$ only the trivial solution $a = (0, 0)$ exists. In particular solution continua cannot cross the value $f = 0$ so that it is sufficient to analyze the bifurcations for positive f . The bifurcations for negative f can be found via the discrete symmetry of (1.1) given by $(a_1, a_2, f) \mapsto (-a_1, -a_2, -f)$.

(b) In principle the exceptional points where the conditions (S) and (T) are not satisfied could be analyzed using different bifurcation theorems. Suitable candidates for a bifurcation theorem in the presence of two-dimensional kernels are the theorems of Healey, Kielhöfer, Krömer [17] and Westreich [24]. Bifurcation results without transversality condition can be found in [18]. However, the required amount of calculations are far too high to justify the use of these theorems in our situation. For the same reason we did not include a detailed analysis of the initial directions of the bifurcation branches which, without any theoretical difficulty, may be calculated using the formulas from section I.6 in Kielhöfer's book [15].

1.2. Frequency combs in physics and engineering. Currently frequency combs are gaining interest as optical sources for high-speed data transmission where the individual comb lines are used as carriers. A high power per combline with the same spectral power distribution is important. An experimental set-up for such frequency combs is given by a microresonator which is coupled to an optical waveguide under the influence of a single, strong, external laser source that is tuned to a resonance wavelength of the device. Inside the resonator the optical intensity is strongly enhanced and modes start to interact in a nonlinear way. As a consequence, the primarily excited mode couples with a multitude of neighboring modes. This leads to a cascaded transfer of power from the pump to the comb lines. Under suitable choice of parameters, a stationary cascade of excited modes can be obtained and results in a stable frequency comb with equidistant spectral lines. If $\hat{a}_k(t)$ denotes the dimensionless complex-valued amplitude of the k -th mode in the microresonator at time t then, following [2, 12], it satisfies the following set of coupled differential equations

$$(1.6) \quad i\partial_t \hat{a}_k(t) = (-i + \zeta)\hat{a}_k(t) + dk^2 \hat{a}_k(t) - \sum_{k', k'' \in \mathbb{Z}} \hat{a}_{k'}(t) \hat{a}_{k''}(t) \bar{\hat{a}}_{k'+k''-k}(t) + i\delta_{0k} f$$

for each $k \in \mathbb{Z}$. In this equation, the parameters ζ, d, f are real and t is normalized time. The term $i\delta_{0k} f$ corresponds to forcing by the external pump, ζ represents the normalized frequency detuning between the source and the principal resonance of the microresonator, and d quantifies the dispersion in the system. The case $d < 0$ corresponds to normal dispersion whereas $d > 0$ is called the anomalous regime, cf. [8, 9]. The loss of power due to radiation and waveguide coupling is modeled by the damping term $-i\hat{a}_k(t)$. In the literature a stationary solution of (1.6) is called a frequency comb.

Via the Fourier series $a(x, t) = \sum_{k \in \mathbb{Z}} \hat{a}_k(t) e^{ikx}$ frequency combs can equally be defined as stationary solutions of the Lugiato-Lefever equation

$$(1.7) \quad i\partial_t a(x, t) = (-i + \zeta)a(x, t) - d\partial_x^2 a(x, t) - |a(x, t)|^2 a(x, t) + if, \quad x \in \mathbb{R}/2\pi\mathbb{Z}, t \in \mathbb{R}.$$

It was originally proposed in [19] as a model for the envelope of a field transmitted through a nonlinearly responding optical cavity. It resembles a nonlinear Schrödinger equation with added damping and forcing. Stationary solutions of (1.7) of the form $a = a_1 + ia_2$ correspond to solutions (a_1, a_2) of (1.1).

The experimental generation of frequency combs in microresonators has been demonstrated many times, cf. the review paper [16]. One of the first demonstrations [6] used a toroidal fused-silica microresonator. In [12] the dynamics of the Kerr comb formation process is experimentally explored and found to be independent of the resonator material system and geometry. One of the first theoretical papers [2] marks the starting point for a series of subsequent investigations and publications. In this paper a numerical simulation of Kerr frequency combs is given based on (1.6), i.e., the modal expansion of the fields. A considerable computational effort is needed to handle the multitude of coupled differential equations. Nevertheless, a detailed account of the temporal dynamics is supplied and analytical expressions (approximations) of the distance of primary comb lines in terms of resonator and pump parameters are derived.

As one can see in Section 5 there are many different shapes of frequency combs. Of particular interest are so-called soliton combs. These are stationary solutions of (1.7) which are highly localized in space. Accordingly their frequency spectrum shows many densely spaced comb lines; cf. Figures 6, 10, 11 and 14. Moreover, the power of the k -th excited frequency in a soliton comb is much higher than the k -th excited frequency in a comb with sparse frequency spectrum, cf. Figure 3. Since these properties of soliton combs are very desirable for high-speed data transmission, they received attention in recent literature. In [3] a numerical study of pump and resonator parameters and their effect on the bandwidth of Kerr combs was performed, and first indications appeared that soliton combs can only be achieved by a special tuning of the pump parameters. According to the simulations presented in [7] these solitons show a high coherence along with a high number of comb lines with flat power distribution. The first experimental proof of soliton combs was done in [11]. The effect of higher order dispersion terms is the topic of [21]. It is shown that incorporating third-order dispersion terms into the model enlarges the parameter ranges where stable soliton combs exist. In [23] the effect of higher order dispersion on the comb shape is discussed.

1.3. Further mathematical results. A rigorous study of the time-dependent problem (1.7) both from the analytical and from the numerical point of view was recently given in [13]. Applying Theorem 2.1 of [13] to the function $a(x, t)e^{i\zeta t}$ one obtains that for $d = 1$ and initial data lying in $H_{\text{per}}^4([0, 2\pi]; \mathbb{C})$ the initial value problem associated to (1.7) admits a unique solution

$$a \in C(\mathbb{R}_+; H_{\text{per}}^4([0, 2\pi]; \mathbb{C})) \cap C^1(\mathbb{R}_+; H_{\text{per}}^2([0, 2\pi]; \mathbb{C})) \cap C^2(\mathbb{R}_+; L_{\text{per}}^2([0, 2\pi]; \mathbb{C}))$$

satisfying the additional bounds $\|a(t)\|_2 \leq C$, $\|a(t)\|_{H^1} \leq C\sqrt{1+t}$ for some positive number $C > 0$ which is independent of t . Furthermore, the paper provides a detailed analysis of the Strang splitting associated to (1.7) including error bounds in $L^2_{\text{per}}([0, 2\pi]; \mathbb{C})$, $H^1_{\text{per}}([0, 2\pi]; \mathbb{C})$ as well as estimates related to the stability properties of the numerical scheme. Further numerical and analytical results related to periodically forced and damped NLS may be found in [1, 10].

1.4. Structure of the paper. The paper is organized as follows. In Section 2 we provide the functional analytical framework for our analysis. This includes an appropriate choice of the function spaces and corresponding solution concepts. In Section 3 the proofs of Theorem 1 (a priori bounds) and Theorem 2 (uniqueness) are given. The proofs of the bifurcation results from Theorem 4 and 5 can be found in Section 4. Section 5 contains illustrations with tables of bifurcation points, bifurcation diagrams and plots of approximate solutions. In the final Section 6 we draw conclusions from our results and formulate some open questions.

1.5. On the generation of the numerical plots. The illustrations in Sections 5.1–5.4 were created with the software package AUTO. It is a free software which determines bifurcation points, approximations of solutions and generates bifurcation diagrams. It can be downloaded from indy.cs.concordia.ca/auto/. We postprocessed the output of AUTO by a MATLAB program to improve the quality of the approximated solutions of (1.1) via several Newton iterations and to compute the Fourier coefficients of the improved approximated solutions. The MATLAB program also produces .pdf files of plotted solutions and their Fourier coefficients. A .zip file containing a README-description and driver files for the code can be downloaded freely from www.waves.kit.edu/downloads/CRC1173_Preprint_2016-7_supplement.zip. By running the driver files AUTO and MATLAB will be invoked and generate all plots of Sections 5.1–5.4.

2. MATHEMATICAL SETUP

First we describe the spaces of solutions in which our analysis works. A weak solution $a \in H^1([0, 2\pi]; \mathbb{R}^2)$ of (1.1) will be called a solution for the sake of simplicity. Notice that every such solution coincides almost everywhere with a smooth classical solution of the equation so that regularity issues will not play a role in the sequel and all solution concepts in fact coincide. In the context of Theorems 1 and 2 it is convenient to consider 2π -periodic classical solutions. For the proof of Theorem 2 the space $H^2_{\text{per}}([0, 2\pi]; \mathbb{R}^2)$ will be useful. In the context of the bifurcation results of Theorems 4 and 5 we consider synchronized solutions of (1.1), i.e. solutions that satisfy additionally $a'(0) = a'(\pi) = 0$. If we set $H := H^1([0, \pi], \mathbb{R}^2)$ then $a = (a_1, a_2)$ is a synchronized solution of (1.1) if and only if $a = (a_1, a_2) \in H$ satisfies

$$\begin{aligned} \int_0^\pi da'_1 \varphi'_1 dx &= \int_0^\pi (-a_2 - \zeta a_1 + (a_1^2 + a_2^2)a_1) \varphi_1 dx && \text{for all } \varphi_1 \in H, \\ \int_0^\pi da'_2 \varphi'_2 dx &= \int_0^\pi (a_1 - \zeta a_2 + (a_1^2 + a_2^2)a_2 - f) \varphi_2 dx && \text{for all } \varphi_2 \in H. \end{aligned}$$

A synchronized solution can be extended evenly around $x = \pi$ and thus produce a 2π -periodic function. This weak setting in the Hilbert space H will be convenient for the proof of the bifurcation results.

Next we describe the trivial (i.e. spatially constant) solutions of (1.1). In order to obtain a global parameterization of the solution curves some new auxiliary parameters t resp. s will be used instead of ζ resp. f . The totality of constant solutions is given next.

Lemma 6. *Let $d \neq 0$ be fixed.*

(a) *Let $f \in \mathbb{R}$ be given. Then the set of constant solutions (a_1, a_2, ζ) of (1.1) is given by $\hat{\Gamma}_f = \{(\hat{a}_1(t), \hat{a}_2(t), \hat{\zeta}(t)) : |t| < 1\}$ where*

$$\hat{a}_1(t) = f(1 - t^2), \quad \hat{a}_2(t) = -ft\sqrt{1 - t^2}, \quad \hat{\zeta}(t) = f^2(1 - t^2) + \frac{t}{\sqrt{1 - t^2}}.$$

(b) *Let $\zeta \in \mathbb{R}$ be given. Then the set of constant solutions (a_1, a_2, f) of (1.1) is given by $\bar{\Gamma}_\zeta = \{(\bar{a}_1(s), \bar{a}_2(s), \bar{f}(s)) : s \in \mathbb{R}\}$ where*

$$\bar{a}_1(s) = \frac{s}{\sqrt{1 + (s^2 - \zeta)^2}}, \quad \bar{a}_2(s) = \frac{s(s^2 - \zeta)}{\sqrt{1 + (s^2 - \zeta)^2}}, \quad \bar{f}(s) = s\sqrt{1 + (s^2 - \zeta)^2}.$$

Proof. Let us first show that constant solutions $a = (a_1, a_2)$ of (1.1) satisfy

$$(2.1) \quad f^2 = |a|^2(1 + (|a|^2 - \zeta)^2).$$

Indeed, for constant solutions (1.1) can be written as

$$\begin{pmatrix} |a|^2 - \zeta & -1 \\ 1 & |a|^2 - \zeta \end{pmatrix} \begin{pmatrix} a_1 \\ a_2 \end{pmatrix} = \begin{pmatrix} 0 \\ f \end{pmatrix}$$

and hence by inverting the matrix

$$(2.2) \quad \begin{pmatrix} a_1 \\ a_2 \end{pmatrix} = \frac{f}{1 + (|a|^2 - \zeta)^2} \begin{pmatrix} 1 \\ |a|^2 - \zeta \end{pmatrix}.$$

Taking the Euclidean norm on both sides of the equation gives (2.1).

Now let us prove (a), so let $f \in \mathbb{R}$ be given and define $t \in (-1, 1)$ via $t(1 - t^2)^{-1/2} = \zeta - |a|^2$. Then (2.1) implies

$$\zeta - t(1 - t^2)^{-1/2} = |a|^2 = \frac{f^2}{1 + t^2(1 - t^2)^{-1}} = f^2(1 - t^2)$$

and hence

$$\zeta = f^2(1 - t^2) + \frac{t}{\sqrt{1 - t^2}}.$$

From the linear system (2.2) and the definition of t we obtain the desired formulas for a_1, a_2 . In order to prove (b) let $\zeta \in \mathbb{R}$ and set $s := \text{sign}(f)|a|$. Then we have

$$f^2 = s^2(1 + (s^2 - \zeta)^2), \quad \text{hence } f = s\sqrt{1 + (s^2 - \zeta)^2}.$$

From the linear system (2.2) and this formula for s we obtain the result. \square

3. PROOF OF THEOREM 1 AND THEOREM 2

We always assume $d \neq 0$ and $f, \zeta \in \mathbb{R}$. We write $\|\cdot\|_p$ for the standard norm on $L^p([0, 2\pi]; \mathbb{R}^2)$ for $p \in [1, \infty]$.

Proof of Theorem 1: We divide the proof into several steps.

Step 1: Here we prove the L^2 -estimate $\|a\|_2 \leq \sqrt{2\pi}|f|$. To this end we define the 2π -periodic function $g : [0, 2\pi] \rightarrow \mathbb{R}$ by

$$g := d(a_2 a_1' - a_1 a_2').$$

By using (1.1) one finds

$$(3.1) \quad g = da_2 a_1'' - da_1 a_2'' = a_2(a_2 + \zeta a_1 - |a|^2 a_1) + a_1(a_1 - \zeta a_2 + |a|^2 a_2 - f) = |a|^2 - f a_1.$$

Since $a_2 a_1' - a_1 a_2'$ is 2π -periodic we obtain

$$0 = \int_0^{2\pi} g \, dx = \int_0^{2\pi} (|a|^2 - f a_1) \, dx \geq \|a\|_2^2 - \sqrt{2\pi}|f|\|a\|_2$$

which implies the desired L^2 -bound

$$(3.2) \quad \|a\|_2 \leq \sqrt{2\pi}|f|.$$

Step 2: Next we prove $|d|\|a'\|_2 \leq 6\pi f^2 \|a\|_2$ and thus $|d|\|a'\|_2 \leq 6\sqrt{2}\pi^{3/2}|f|^3$ due to (3.2). Using the differential equation (1.1) we get

$$\begin{aligned} |d|\|a'\|_2^2 &= |d| \int_0^{2\pi} a_1' (-da_2'' + \zeta a_2 - |a|^2 a_2 + f)' \, dx + a_2' (da_1'' - \zeta a_1 + |a|^2 a_1)' \, dx \\ &= |d|d \int_0^{2\pi} (a_2' a_1''' - a_1' a_2''') \, dx + |d| \int_0^{2\pi} a_1' (-|a|^2 a_2)' + a_2' (|a|^2 a_1)' \, dx \\ &= |d|d \int_0^{2\pi} (a_2' a_1'' - a_1' a_2'')' \, dx + |d| \int_0^{2\pi} (-a_2 a_1' + a_1 a_2') (|a|^2)' \, dx \\ (3.3) \quad &= 0 + |d| \int_0^{2\pi} (a_2 a_1' - a_1 a_2')' |a|^2 \, dx \\ &\leq \int_0^{2\pi} |g| |a|^2 \, dx \\ &\leq \|g\|_\infty \|a\|_2^2 \\ &\stackrel{(3.2)}{\leq} \sqrt{2\pi}|f| \|g\|_\infty \|a\|_2. \end{aligned}$$

Note that g is the derivative of a 2π -periodic function and therefore satisfies $\int_0^{2\pi} g \, dx = 0$. Hence there exists $x_0 \in [0, 2\pi]$ such that $g(x_0) = 0$ and the supremum norm of g can be

estimated as follows

$$\begin{aligned}
\|g\|_\infty &\leq \sup_{x \in [0, 2\pi]} |g(x) - g(x_0)| \\
&\leq \int_0^{2\pi} |g'| dx \\
&\stackrel{(3.1)}{\leq} \int_0^{2\pi} 2|a'| |a| + |f| |a'_1| dx \\
&\leq (2\|a\|_2 + \sqrt{2\pi}|f|) \|a'\|_2 \\
&\stackrel{(3.2)}{\leq} 3\sqrt{2\pi}|f| \|a'\|_2.
\end{aligned}$$

By our previous estimates (3.3) and (3.2) this gives

$$(3.4) \quad |d| \|a'\|_2 \leq \sqrt{2\pi}|f| \|a\|_2 \cdot 3\sqrt{2\pi}|f| = 6\pi f^2 \|a\|_2 \leq 6\sqrt{2\pi}^{3/2} |f|^3$$

which finishes step 2.

Step 3: Now we show the first of two L^∞ -bounds: $\|a\|_\infty \leq |f|(1 + 12\pi^2 f^2 |d|^{-1})$. From the L^2 -estimate (3.2) we infer that there is an $x_1 \in I$ satisfying $|a(x_1)| \leq |f|$. Hence our first L^∞ -estimate follows from

$$\begin{aligned}
\|a\|_\infty &\leq |a(x_1)| + \|a - a(x_1)\|_\infty \\
&\leq |f| + \|a'\|_1 \\
(3.5) \quad &\leq |f| + \sqrt{2\pi} \|a'\|_2 \\
&\stackrel{(3.4)}{\leq} |f| + \sqrt{2\pi} \cdot 6\sqrt{2\pi}^{3/2} |f|^3 |d|^{-1} \\
&= |f|(1 + 12\pi^2 f^2 |d|^{-1}).
\end{aligned}$$

Step 4: Next we show

$$(3.6) \quad \|a\|_2 \leq (-\zeta \operatorname{sign}(d) - \gamma(d, f))^{-1} \sqrt{2\pi} |f|.$$

whenever $-\zeta \operatorname{sign}(d) - \gamma(d, f) > 0$ for $\gamma(d, f)$ from (1.3). Testing (1.1) with (a_1, a_2) and adding up the resulting equations yields

$$(3.7) \quad d \|a'\|_2^2 = -\zeta \|a\|_2^2 + \|a\|_4^4 - f \int_0^{2\pi} a_2 dx.$$

This can be used in the following way.

$$\begin{aligned}
36\pi^2 f^4 |d|^{-1} \|a\|_2^2 &= |d|^{-1} (6\pi f^2 \|a\|_2)^2 \\
(3.8) \quad &\stackrel{(3.4)}{\geq} |d|^{-1} (|d| \|a'\|_2)^2 \\
&= |d| \|a'\|_2^2 \\
&\stackrel{(3.7)}{=} -\zeta \operatorname{sign}(d) \|a\|_2^2 + \operatorname{sign}(d) \|a\|_4^4 - \operatorname{sign}(d) f \int_0^{2\pi} a_2 dx.
\end{aligned}$$

In order to prove (3.6) we first suppose $d > 0$. Then (3.8) implies

$$36\pi^2 f^4 |d|^{-1} \|a\|_2^2 \geq -\zeta \|a\|_2^2 - \sqrt{2\pi} |f| \|a\|_2$$

from which we infer the desired bound

$$\sqrt{2\pi} |f| \geq (-\zeta - 36\pi^2 f^4 |d|^{-1}) \|a\|_2 = (-\zeta - \gamma(d, f)) \|a\|_2.$$

Supposing now $d < 0$ we find that (3.8) implies

$$\begin{aligned} 36\pi^2 f^4 |d|^{-1} \|a\|_2^2 &\geq (\zeta - \|a\|_\infty^2) \|a\|_2^2 - \sqrt{2\pi} |f| \|a\|_2 \\ &\stackrel{(3.5)}{\geq} (\zeta - f^2(1 + 12\pi^2 f^2 |d|^{-1})^2) \|a\|_2^2 - \sqrt{2\pi} |f| \|a\|_2 \end{aligned}$$

from which we obtain

$$\sqrt{2\pi} |f| \geq (\zeta - 36\pi^2 f^4 |d|^{-1} - f^2(1 + 12\pi^2 f^2 |d|^{-1})^2) \|a\|_2 = (\zeta - \gamma(d, f)) \|a\|_2.$$

so that (3.6) is proved.

Step 5: Finally, we show

$$\|a\|_\infty \leq (-\zeta \operatorname{sign}(d) - \gamma(d, f))^{-1} |f| (1 + 12\pi^2 f^2 |d|^{-1}).$$

$-\zeta \operatorname{sign}(d) - \gamma(d, f) > 0$. This completes the proof of Theorem 1. The L^2 -estimate from Step 4 entails, just as in Step 3, that there exists some $x_1 \in [0, 2\pi]$ such that $|a(x_1)| \leq (-\zeta \operatorname{sign}(d) - \gamma(d, f))^{-1} |f|$ and the claim follows from

$$\begin{aligned} \|a\|_\infty &\leq |a(x_1)| + \sqrt{2\pi} \|a'\|_2 \\ &\stackrel{(3.4)}{\leq} |a(x_1)| + 6\pi \sqrt{2\pi} f^2 |d|^{-1} \|a\|_2 \\ &\leq \frac{|f|(1 + 12\pi^2 f^2 |d|^{-1})}{-\zeta \operatorname{sign}(d) - \gamma(d, f)} \quad \text{by Step 4.} \end{aligned}$$

Now we come to the proof of the uniqueness result from Theorem 2. Let us first outline our strategy to prove the result. We use the fact that a solution $a = (a_1, a_2) : [0, 2\pi] \rightarrow \mathbb{R} \times \mathbb{R}$ of (1.1) is constant if and only if the function $A = (A_1, A_2) := (a'_1, a'_2)$ is trivial. Since (a_1, a_2) solves (1.1) the functions A_1, A_2 satisfy the boundary value problem

$$\begin{aligned} (3.9) \quad -dA_1'' &= -A_2 - \zeta A_1 + (3a_1^2 + a_2^2)A_1 + 2a_1 a_2 A_2, \\ -dA_2'' &= A_1 - \zeta A_2 + 2a_1 a_2 A_1 + (a_1^2 + 3a_2^2)A_2, \\ A_1, A_2 & \text{ } 2\pi\text{-periodic.} \end{aligned}$$

In view of (3.9) it is natural to study the operator

$$L_{d,\zeta} : \begin{cases} H_{\text{per}}^2([0, 2\pi]; \mathbb{R}^2) &\rightarrow L^2([0, 2\pi]; \mathbb{R}^2), \\ (B_1, B_2) &\mapsto (-dB_1'' + \zeta B_1 + B_2, -dB_2'' + \zeta B_2 - B_1). \end{cases}$$

Using the fact that the embedding $\operatorname{Id} : H_{\text{per}}^2([0, 2\pi]; \mathbb{R}^2) \rightarrow L^2([0, 2\pi]; \mathbb{R}^2)$ is compact we obtain the following result.

Lemma 7. *The operator $L_{d,\zeta}$ has a bounded inverse $L_{d,\zeta}^{-1} : L^2([0, 2\pi]; \mathbb{R}^2) \rightarrow H_{\text{per}}^2([0, 2\pi]; \mathbb{R}^2)$ with the property that $\text{Id} \circ L_{d,\zeta}^{-1} : L^2([0, 2\pi]; \mathbb{R}^2) \rightarrow L^2([0, 2\pi]; \mathbb{R}^2)$ is compact and $\|\text{Id} \circ L_{d,\zeta}^{-1}\| \leq \min\{1, (\text{sign}(d)\zeta)_+^{-1}\}$.*

Proof. Let $(B_1, B_2) \in H_{\text{per}}^2([0, 2\pi]; \mathbb{R}^2)$ and $(g_1, g_2) \in L^2([0, 2\pi]; \mathbb{R}^2)$ satisfy the equation $L_{d,\zeta}(B_1, B_2) = (g_1, g_2)$, i.e., $-dB_1'' + \zeta B_2 + B_2 = g_1$ and $-dB_2'' + \zeta B_2 - B_1 = g_2$. Testing these differential equations with (B_1, B_2) respectively $(B_2, -B_1)$ and adding up the resulting equations yields

$$(3.10) \quad d(\|B_1'\|_2^2 + \|B_2'\|_2^2) + \zeta(\|B_1\|_2^2 + \|B_2\|_2^2) = \int_0^{2\pi} (g_1 B_1 + g_2 B_2) dx,$$

$$(3.11) \quad \|B_1\|_2^2 + \|B_2\|_2^2 = \int_0^{2\pi} (g_1 B_2 - g_2 B_1) dx.$$

The second line (3.11) shows that $L_{d,\zeta}$ is injective. Moreover, using $\|B_1'\|_2^2 + \|B_2'\|_2^2 \geq 0$ as well as Hölder's inequality we obtain from (3.10) and (3.11)

$$\max\{1, \text{sign}(d)\zeta\} \|(B_1, B_2)\|_2^2 \leq \|(g_1, g_2)\|_2 \|(B_1, B_2)\|_2$$

and thus

$$\|(B_1, B_2)\|_2 \leq \min\{1, (\text{sign}(d)\zeta)_+^{-1}\} \|(g_1, g_2)\|_2.$$

From this and (3.10) we get the estimate

$$|d| \|(B_1', B_2')\|_2^2 \leq (1 + |\zeta|) \|(g_1, g_2)\|_2^2$$

and using the differential equation and the L^2 -estimate on (B_1, B_2) we find

$$|d| \|(B_1'', B_2'')\|_2 \leq (2 + |\zeta|) \|(g_1, g_2)\|_2.$$

This proves the bounded invertibility of $L_{d,\zeta}$ as well as the norm estimate for $\text{Id} \circ L_{d,\zeta}^{-1}$. \square

Proof of Theorem 2: If (A_1, A_2) satisfies (3.9) then we have $(A_1, A_2) = K_a(A_1, A_2)$ where $K_a : L^2([0, 2\pi]; \mathbb{R}^2) \rightarrow L^2([0, 2\pi]; \mathbb{R}^2)$ is given by

$$(3.12) \quad K_a \begin{pmatrix} A_1 \\ A_2 \end{pmatrix} := \text{Id} \circ L_{d,\zeta}^{-1} \left(M_a \begin{pmatrix} A_1 \\ A_2 \end{pmatrix} \right) \text{ with } M_a = \begin{pmatrix} 3a_1^2 + a_2^2 & 2a_1 a_2 \\ 2a_1 a_2 & a_1^2 + 3a_2^2 \end{pmatrix}.$$

Hence, it suffices to prove that the operator norm $\|K_a\|$ is less than 1 whenever $\text{sign}(d)\zeta > \zeta^*$ or $\text{sign}(d)\zeta < \zeta_*$. Consider the matrix M_a as a map from $L^2([0, 2\pi]; \mathbb{R}^2)$ into itself. Then its operator norm is bounded as follows

$$\|M_a\| \leq \left\| \begin{pmatrix} 4\|a\|_\infty^2 & 2\|a\|_\infty^2 \\ 2\|a\|_\infty^2 & 4\|a\|_\infty^2 \end{pmatrix} \right\| = \|a\|_\infty^2 \cdot \left\| \begin{pmatrix} 4 & 2 \\ 2 & 4 \end{pmatrix} \right\| = 6\|a\|_\infty^2,$$

since the largest eigenvalue of $\begin{pmatrix} 4 & 2 \\ 2 & 4 \end{pmatrix}$ is 6. Combining this inequality with the estimate from Lemma 7 we get

$$\|K_a\| \leq 6 \min\{1, (\text{sign}(d)\zeta)_+^{-1}\} \|a\|_\infty^2.$$

In the first case, where $\text{sign}(d)\zeta > \zeta^* > 0$, Theorem 1 gives, by choice of ζ^* ,

$$\|K_a\| \leq 6(\text{sign}(d)\zeta)^{-1} \|a\|_\infty^2 < 6(\zeta^*)^{-1} f^2 (1 + 12\pi^2 f^2 |d|^{-1})^2 = 1.$$

In the second case, where $\text{sign}(d)\zeta < \zeta_* < 0$ and in particular $-\zeta \text{sign}(d) - \gamma(d, f) > 0$, we get from Theorem 1 and again by the choice of ζ_*

$$\|K_a\| \leq 6\|a\|_\infty^2 \leq \left(\frac{\sqrt{6}|f|(1 + 12\pi^2 f^4 |d|^{-1})}{-\zeta \text{sign}(d) - \gamma(d, f)} \right)^2 < \left(\frac{\sqrt{6}|f|(1 + 12\pi^2 f^4 |d|^{-1})}{-\zeta_* - \gamma(d, f)} \right)^2 = 1$$

which is all we had to show. \square

4. PROOF OF THEOREM 4 AND THEOREM 5

In this section we prove the bifurcation results for the Lugiato-Lefever equation (1.1). We will always assume that $d \neq 0$ is fixed. As explained earlier our sufficient conditions for bifurcation from constant solutions of (1.1) will be established in the context of the Neumann boundary value problem

$$(4.1) \quad \begin{aligned} -da_1'' &= -a_2 - \zeta a_1 + (a_1^2 + a_2^2)a_1, & a_1'(0) &= a_1'(\pi) = 0, \\ -da_2'' &= a_1 - \zeta a_2 + (a_1^2 + a_2^2)a_2 - f, & a_2'(0) &= a_2'(\pi) = 0. \end{aligned}$$

In this way the shift-invariance of the general 2π -periodic system is circumvented. Using the notation introduced in the introduction we will find the existence of synchronized solution branches bifurcating from the curves of constant solutions.

Let us now shortly outline how our bifurcation analysis is organized. In Section 4.1 we first provide a functional analytical framework for solutions of (4.1). The construction of solutions is done with the help of the bifurcation theorem due to Crandall and Rabinowitz (Theorem 8). In Theorem 4, the family of trivial solutions will be $\hat{\Gamma}_f$ for fixed $f \in \mathbb{R}$ and in Theorem 5 it will be $\bar{\Gamma}_\zeta$ for fixed $\zeta \in \mathbb{R}$. The proof of these theorems is accomplished in four steps. In Section 4.2 we first determine the candidates for the bifurcation points of (1.1) with respect to $\hat{\Gamma}_f, \bar{\Gamma}_\zeta$ proving Theorem 4(i), Theorem 5(i). This result will be used in Section 4.3 to establish the upper bounds for the number of bifurcation points claimed in Theorem 4(ii) and Theorem 5(ii). In order to prove the existence of bifurcating branches it remains to check the hypotheses of the Crandall-Rabinowitz theorem in the context of the Neumann boundary value problem (4.1). In Section 4.4 we show that the kernels at the possible bifurcation points (calculated in Section 4.2) are simple if the conditions (S) from the respective theorem holds. In the same way the transversality condition will be verified in Section 4.5 supposing that condition (T) holds. Hence, a direct application of Theorem 8 establishes the existence of local curves containing nontrivial solutions of (4.1) that emanate from $\hat{\Gamma}_f, \bar{\Gamma}_\zeta$ respectively. Considering (4.1) as an equation in the space of $2\pi/k$ -periodic functions one even finds that the uniquely determined bifurcating branch from bifurcation points associated to k via (1.4) resp. (1.5) locally consists of $2\pi/k$ -periodic solutions. Notice that this is possible due to the fact that the functions in the kernel of the linearized operator are $2\pi/k$ -periodic, see (4.4) in Proposition 10. Moreover, the a priori bounds for a from Theorem 1 and the uniqueness result from Theorem 2 tell us that for any given $f \in \mathbb{R}$ the continua emanating from $\hat{\Gamma}_f$ must be bounded with respect to both variables a, ζ so that Rabinowitz' global bifurcation theorem [22] yields that each continuum returns to $\hat{\Gamma}_f$ at another point. Hence, part (iii) of Theorem 4 and Theorem 5 is shown and the proof is complete.

4.1. Functional analytical framework and preliminaries.

We look for solutions of (4.1) in the function space $H := H^1([0, \pi]; \mathbb{R}^2)$. It is a Hilbert space with the inner product $\langle \cdot, \cdot \rangle_H$ given by

$$\langle \varphi, \psi \rangle_H := \int_0^\pi |d|(\varphi'_1 \psi'_1 + \varphi'_2 \psi'_2) + \varphi_1 \psi_1 + \varphi_2 \psi_2 dx \quad \text{for } \varphi = \begin{pmatrix} \varphi_1 \\ \varphi_2 \end{pmatrix}, \psi = \begin{pmatrix} \psi_1 \\ \psi_2 \end{pmatrix} \in H.$$

If $D : \text{dom}(D) \rightarrow \mathbb{R}$ denotes the selfadjoint realization of the differential operator $\varphi \mapsto -|d|\varphi'' + \varphi$ with homogeneous Neumann boundary values at $0, \pi$ then $\langle \varphi, \psi \rangle_H = \langle D\varphi, \psi \rangle_{L^2}$ for all $\varphi \in \text{dom}(D)$. Even though it will not be used in the sequel let us state without proof

$$\text{dom}(D) = \left\{ \varphi \in H^2([0, \pi]; \mathbb{R}^2) : \varphi'(0) = \varphi'(\pi) = \begin{pmatrix} 0 \\ 0 \end{pmatrix} \right\}.$$

The operator D has a compact inverse $D^{-1} : H \rightarrow \text{dom}(D) \subset H$ so that (4.1) may be rewritten as $G(a, \zeta, f) = 0$ where the function $G : H \times \mathbb{R} \times \mathbb{R} \rightarrow H$ is given by

$$(4.2) \quad G(a, \zeta, f) := \text{sign}(d)a - D^{-1} \left(-\zeta a + \text{sign}(d)a + |a|^2 a + \begin{pmatrix} -a_2 \\ a_1 \end{pmatrix} + \begin{pmatrix} 0 \\ -f \end{pmatrix} \right).$$

In order to prove bifurcation results from the family of constant solutions of (4.1) let us recall the Crandall-Rabinowitz bifurcation theorem.

Theorem 8 (Crandall-Rabinowitz [4]). *Let $I \subset \mathbb{R}$ be an open interval and let $F : H \times I \rightarrow H$ be twice continuously differentiable such that $F(0, \lambda) = 0$ for all $\lambda \in I$ and such that $F_x(0, \lambda_0)$ is an index-zero Fredholm operator for $\lambda_0 \in I$. Moreover assume:*

- (H1) *there is $\varphi \in H, \varphi \neq 0$ such that $\ker(F_x(0, \lambda_0)) = \text{span}\{\varphi\}$,*
- (H2) *$\langle F_{x\lambda}(0, \lambda_0)[\varphi], \varphi^* \rangle_H \neq 0$ where $\ker(F_x(0, \lambda_0)^*) = \text{span}\{\varphi^*\}$.*

Then there exists $\epsilon > 0$ and a continuously differentiable curve $(x, \lambda) : (-\epsilon, \epsilon) \rightarrow H \times \mathbb{R}$ with $\lambda(0) = \lambda_0, x(0) = 0, x'(0) = \varphi$ and $x(t) \neq 0$ for $0 < |t| < \epsilon$ and $F(x(t), \lambda(t)) = 0$ for all $t \in (-\epsilon, \epsilon)$. Moreover, there exists a neighbourhood $U \times J \subset H \times I$ of $(0, \lambda_0)$ such that all nontrivial solutions in $U \times J$ of $F(x, \lambda) = 0$ lie on the curve.

In the proof of Theorem 4 and Theorem 5 we will apply Theorem 8 to the functions $\hat{F} : H \times (-1, 1) \rightarrow H$ and $\bar{F} : H \times \mathbb{R} \rightarrow H$ given by

$$(4.3) \quad \begin{aligned} \hat{F}(b, t) &:= G(b + \hat{a}(t), \hat{\zeta}(t), f), & b \in H, t \in (-1, 1), \\ \bar{F}(b, s) &:= G(b + \bar{a}(s), \zeta, \bar{f}(s)), & b \in H, s \in \mathbb{R} \end{aligned}$$

where the trivial solution curves $(\hat{a}(t), \hat{\zeta}(t))$ respectively $(\bar{a}(s), \zeta(s))$ are taken from Lemma 6. Checking the assumptions of Theorem 8 requires the calculation of the derivatives of \hat{F}, \bar{F} at the trivial solutions. The necessary preparations are made in the following proposition.

Proposition 9. *Let $a \in H$, $\zeta, f \in \mathbb{R}$ and set*

$$N(a, \zeta) = \begin{pmatrix} -\zeta + 3a_1^2 + a_2^2 & -1 + 2a_1a_2 \\ 1 + 2a_1a_2 & -\zeta + a_1^2 + 3a_2^2 \end{pmatrix},$$

$$M_1(a) = \begin{pmatrix} 6a_1 & 2a_2 \\ 2a_2 & 2a_1 \end{pmatrix}, \quad M_2(a) = \begin{pmatrix} 2a_2 & 2a_1 \\ 2a_1 & 6a_2 \end{pmatrix}.$$

Then we have for all $\varphi, \psi \in H$

$$G_a(a, \zeta, f)[\varphi] = \text{sign}(d)\varphi - D^{-1}(N(a, \zeta)\varphi + \text{sign}(d)\varphi),$$

$$G_{aa}(a, \zeta, f)[\varphi, \psi] = -D^{-1} \begin{pmatrix} \varphi^T M_1(a)\psi \\ \varphi^T M_2(a)\psi \end{pmatrix}$$

as well as

$$G_\zeta(a, \zeta, f) = D^{-1}a, \quad G_f(a, f) = D^{-1}(0, 1)^T,$$

$$G_{a\zeta}(a, \zeta, f)[\varphi] = D^{-1}\varphi, \quad G_{af}(a, \zeta, f)[\varphi] = 0.$$

The proof of Proposition 9 is mere calculation and will therefore be dropped. In the next proposition we characterize $\ker(G_a(a, \zeta, f))$ and $\ker(G_a(a, \zeta, f)^*)$ at a constant solution $a \in \mathbb{R}^2 \subset H$ of (4.1).

Proposition 10. *Let $\zeta, f \in \mathbb{R}$. Then for every constant solution $a = (a_1, a_2) \in \mathbb{R}^2 \subset H$ of (4.1) we have*

$$(4.4) \quad \ker(G_a(a, \zeta, f)) = \text{span}\{\varphi_k(a) : k \in \mathbb{N}_0 \text{ satisfies (4.6)}\},$$

$$(4.5) \quad \ker(G_a(a, \zeta, f)^*) = \text{span}\{\varphi_k^*(a) : k \in \mathbb{N}_0 \text{ satisfies (4.6)}\},$$

where

$$(4.6) \quad (\zeta + dk^2)^2 - 4|a|^2(\zeta + dk^2) + 1 + 3|a|^4 = 0$$

and

$$\varphi_k(a)(x) = \alpha^k \cos(kx), \quad \varphi_k^*(a)(x) = \beta^k \cos(kx) \quad \text{with } \alpha^k, \beta^k \in \mathbb{R}^2 \text{ given by}$$

$$(4.7) \quad \alpha^k = \begin{cases} \begin{pmatrix} 1 - 2a_1a_2 \\ 3a_1^2 + a_2^2 - \zeta - dk^2 \\ a_1^2 + 3a_2^2 - \zeta - dk^2 \\ -1 - 2a_1a_2 \end{pmatrix} & \text{if } a_1a_2 \neq \frac{1}{2} \quad \text{or} \quad 3a_1^2 + a_2^2 \neq \zeta + dk^2, \\ \begin{pmatrix} a_1^2 + 3a_2^2 - \zeta - dk^2 \\ -1 - 2a_1a_2 \end{pmatrix} & \text{if } a_1a_2 = \frac{1}{2} \quad \text{and} \quad 3a_1^2 + a_2^2 = \zeta + dk^2, \end{cases}$$

$$(4.8) \quad \beta^k = \begin{cases} \begin{pmatrix} -1 - 2a_1a_2 \\ 3a_1^2 + a_2^2 - \zeta - dk^2 \\ a_1^2 + 3a_2^2 - \zeta - dk^2 \\ 1 - 2a_1a_2 \end{pmatrix} & \text{if } a_1a_2 \neq -\frac{1}{2} \quad \text{or} \quad 3a_1^2 + a_2^2 \neq \zeta + dk^2, \\ \begin{pmatrix} a_1^2 + 3a_2^2 - \zeta - dk^2 \\ 1 - 2a_1a_2 \end{pmatrix} & \text{if } a_1a_2 = -\frac{1}{2} \quad \text{and} \quad 3a_1^2 + a_2^2 = \zeta + dk^2. \end{cases}$$

Proof. By Proposition 9 every function $\varphi \in \ker(G_a(a, \zeta, f))$ satisfies $-d\varphi'' = N(a, \zeta)\varphi$ in $(0, \pi)$ and $\varphi'(0) = \varphi'(\pi) = 0$. From the Fourier series expansion

$$(4.9) \quad \varphi(x) = \sum_{k \in \mathbb{N}_0} \alpha^k \cos(kx) \quad \text{for } x \in [0, \pi]$$

we obtain the equation

$$\sum_{k \in \mathbb{N}_0} (dk^2 \text{Id} - N(a, \zeta)) \alpha^k \cos(kx) = 0 \quad \text{for } x \in [0, \pi].$$

Hence, for all $k \in \mathbb{N}_0$ the vector α^k lies in the kernel of the matrix

$$dk^2 \text{Id} - N(a, \zeta) = \begin{pmatrix} \zeta + dk^2 - 3a_1^2 - a_2^2 & 1 - 2a_1a_2 \\ -1 - 2a_1a_2 & \zeta + dk^2 - a_1^2 - 3a_2^2 \end{pmatrix}.$$

This implies that $\ker(G_a(a, \zeta, f))$ is nontrivial if and only if the determinant of one of these matrices vanishes. Calculating $\det(dk^2 \text{Id} - N(a, \zeta))$ for all $k \in \mathbb{N}_0$ we obtain that $\ker(G_a(a, \zeta, f))$ is nontrivial if and only if there is a solution $k \in \mathbb{N}_0$ of (4.6). In that case the kernel of $dk^2 \text{Id} - N(a, \zeta)$ is spanned by the vector $\varphi_k(a)$ given by (4.7) which proves the formula for $\ker(G_a(a, \zeta, f))$ from (4.4). A similar calculation shows that $\varphi^* \in \ker(G_a(a, \zeta, f)^*)$ satisfies $-d\varphi^{*''} = N(a, \zeta)^T \varphi^*$ in $(0, \pi)$ and $\varphi^{*'}(0) = \varphi^{*'}(\pi) = 0$. From this the formula (4.5) for $\ker(G_a(a, \zeta, f)^*)$ follows as above. \square

Since for every given $\zeta, f \in \mathbb{R}$ equation (4.6) has at most two different solutions $k_1, k_2 \in \mathbb{N}_0$ we know that the spaces $\ker(G_a(a, \zeta, f))$ are at most two-dimensional. In the following proposition we single out those parameters for which we have one-dimensional kernels.

Proposition 11. *Let ζ, f, a be chosen as in Proposition 10 such that (4.6) holds for some $k \in \mathbb{N}_0$. Then $\ker(G_a(a, \zeta, f))$ and $\ker(G_a(a, \zeta, f)^*)$ are one-dimensional if and only if*

$$-k^2 + d^{-1}(4|a|^2 - 2\zeta) \neq j^2 \quad \text{for all } j \in \mathbb{N}_0 \setminus \{k\}.$$

Proof. Let $\ker(G_a(a, \zeta, f))$ contain two linearly independent nontrivial vectors. Proposition 10 then implies that equation (4.6) has a second solution $j \in \mathbb{N}_0$ which gives

$$(\zeta + dk^2)^2 - 4(\zeta + dk^2)|a|^2 = (\zeta + dj^2)^2 - 4(\zeta + dj^2)|a|^2 \quad \text{and} \quad \zeta + dk^2 \neq \zeta + dj^2.$$

From this we infer $2\zeta + dk^2 + dj^2 = 4|a|^2$ or equivalently

$$-k^2 + d^{-1}(4|a|^2 - 2\zeta) = j^2 \quad \text{for some } j \in \mathbb{N}_0 \setminus \{k\}.$$

Vice versa, by (4.4), this condition implies that $\ker(G_a(a, \zeta, f))$ is two-dimensional and the result follows. \square

Remark. The applicability of the Crandall-Rabinowitz Theorem relies on the simplicity of the kernel of the linearized equation, which we will check using Proposition 11. In the setting of 2π -periodic functions simplicity of the kernel of the linearized equation never holds. This can be seen as follows: First notice that (4.6), which is a necessary condition for bifurcation for the Neumann problem (4.1), is also a necessary condition for bifurcation for the 2π -periodic problem (1.1). The proof from above only needs small changes: the operator $D\varphi := (-|d|\varphi_1'' +$

$\varphi_1, -|d|\varphi_2'' + \varphi_2)$, now equipped with periodic boundary conditions on $[0, 2\pi]$, has a compact inverse $D^{-1} : H_{\text{per}} \rightarrow H_{\text{per}}$ where H_{per} denotes the restriction of 2π -periodic functions from $H^1(\mathbb{R}; \mathbb{R}^2)$ to the interval $(0, 2\pi)$. Furthermore, in the Fourier series expansion (4.9) the terms $\tilde{\alpha}^k \sin(kx)$ with vectors $\tilde{\alpha}^k \in \mathbb{R}^2$ additionally occur. The vanishing of $\det(dk^2 \text{Id} - N(a, \zeta))$ then appears in the same way as a necessary condition for the nontrivial solvability of the linear equation $-d\varphi'' = N(a, \zeta)\varphi$ by a 2π -periodic function φ . However, with $\alpha^k \cos(kx)$ belonging to the $\ker(G_a(a, \zeta, f))$ for some $k \in \mathbb{N}$ also $\alpha^k \sin(kx)$ belongs to the kernel making it at least two-dimensional. This is one of the reasons why we chose to consider synchronized solutions rather than periodic solutions.

4.2. Determination of all possible bifurcation points.

First let us mention that the solutions of (4.6) for $k = 0$ do not give rise to bifurcation from $\hat{\Gamma}_f, \bar{\Gamma}_\zeta$ regardless of whether the assumptions (S),(T) are satisfied. This is not in contradiction with the Crandall-Rabinowitz Theorem for the following reason. In our analysis we use the parameterizations of $\hat{\Gamma}_f, \bar{\Gamma}_\zeta$ from Lemma 6 having the property that $t \mapsto \hat{\zeta}(t), s \mapsto \bar{f}(s)$ may not be injective for some parameter samples. In our bifurcation analysis related to $k = 0$ this inconvenience leads to a false prediction of bifurcation in the following way. In order to keep the explanations short we explain the situation only for the bifurcation analysis related to $\hat{\Gamma}_f$. Since we use t (and not ζ) as the parameter in the Crandall-Rabinowitz theorem we find a bifurcating branch w.r.t. t whenever (4.6) as well as (S) and (T) are satisfied for some $k \in \mathbb{N}_0$ and some $t_0 \in (-1, 1)$. One can check that in the special case $k = 0$ this is equivalent to saying that the curve $\hat{\zeta}$ has a turning point at t_0 , i.e. we have $\hat{\zeta}'(t_0) = 0, \hat{\zeta}''(t_0) \neq 0$. As a consequence, for any given ε close enough to 0 there is a value δ_ε converging to 0 as $\varepsilon \rightarrow 0$ such that $\delta_\varepsilon \cdot \varepsilon < 0$ and $\hat{\zeta}(t_0 + \varepsilon) = \hat{\zeta}(t_0 + \delta_\varepsilon)$. Hence the bifurcation theorem detects the branch $(t_0 + \varepsilon, \hat{a}(t_0 + \delta_\varepsilon))$ bifurcating from $(t_0 + \varepsilon, \hat{a}(t_0 + \varepsilon))$ at $\varepsilon = 0$. Clearly, $(\hat{\zeta}(t_0 + \varepsilon), \hat{a}(t_0 + \delta_\varepsilon)) = (\hat{\zeta}(t_0 + \delta_\varepsilon), \hat{a}(t_0 + \delta_\varepsilon))$ still lies on $\hat{\Gamma}_f$ and so this branch bifurcates with respect to the variable t , but not with respect to ζ .

For that reason the case $k = 0$ will be left aside when we determine the possible bifurcation points. Note that this phenomenon could be avoided if we locally parameterized the trivial solution families $\hat{\Gamma}_f$ by ζ . However, since this parameterization is in general not global further technical complications would arise.

In Theorem 4: For given $f \in \mathbb{R}$ we have to determine all $t \in (-1, 1)$ such that $\hat{F}_a(0, t) = G_a(\hat{a}(t), \hat{\zeta}(t), f)$ has a nontrivial kernel. According to Proposition 10 this is the case if and only if there is $k \in \mathbb{N}_0$ such that

$$(4.10) \quad (\hat{\zeta}(t) + dk^2 - 2|\hat{a}(t)|^2)^2 = |\hat{a}(t)|^4 - 1.$$

In particular this implies $1 \leq |\hat{a}(t)|^2 = f^2(1 - t^2)$ (see Lemma 6) so that $|f| \geq 1$ is a necessary condition for bifurcation from $\hat{\Gamma}_f$. Furthermore, in case $|f| \geq 1$, we obtain from the formulas for $\hat{a}(t), \hat{\zeta}(t)$ (see Lemma 6) and (4.10)

$$|t| \leq 1 - |f|^{-2} \quad \text{and} \quad dk^2 = f^2(1 - t^2) - \frac{t}{\sqrt{1 - t^2}} - \sigma \sqrt{f^4(1 - t^2)^2 - 1}$$

for some $\sigma \in \{-1, 1\}$ so that part (i) of Theorem 4 is proved.

In Theorem 5: Now let $\zeta \in \mathbb{R}$ be fixed. Proposition 10 and $|\bar{a}(s)|^2 = s^2$ imply that the operator $\bar{F}_a(0, s) = G_a(\bar{a}(s), \zeta, \bar{f}(s))$ has a nontrivial kernel if and only if

$$(\zeta + dk^2 - 2s^2)^2 = s^4 - 1.$$

This implies $(\zeta + dk^2)^2 \geq 3$ and $s^2 = \frac{2}{3}(\zeta + dk^2) - \frac{\sigma}{3}((\zeta + dk^2)^2 - 3)^{1/2}$ for some $\sigma \in \{-1, 1\}$. From the nonnegativity of s^2 we infer $\zeta + dk^2 \geq 0$ and thus $\zeta + dk^2 \geq \sqrt{3}$. Hence, $|s|$ is given by the formula (1.5) for $\sigma \in \{-1, 1\}$ and part (i) of Theorem 5 is proved.

4.3. Number of bifurcation points.

In Theorem 4: We have to prove that for all $f \in \mathbb{R}$ the trivial solution family $\hat{\Gamma}_f$ contains at most $\hat{k}(f)$ bifurcation points where $\hat{k}(f)$ was defined in Theorem 4 (ii). By Proposition 10 every bifurcation point $(a, \zeta) \in \hat{\Gamma}_f$ satisfies the quadratic equation (4.6) for some $k \in \mathbb{N}$. Hence every k gives rise to at most two bifurcation points and therefore it suffices to prove $2k \leq \hat{k}(f)$. Formula (4.6) implies

$$0 \leq (\zeta + dk^2 - 2|a|^2)^2 = |a|^4 - 1.$$

This shows that bifurcation can only occur if $|a| \geq 1$ and together with (2.1) we get

$$f^2 \geq |a|^2 \quad \text{and} \quad f^2 \geq 1 + (|a|^2 - \zeta)^2.$$

Substituting ζ from (4.6) we obtain $\zeta + dk^2 - 2|a|^2 = \pm\sqrt{|a|^4 - 1}$ and thus

$$\begin{aligned} |d|k^2 &\leq |dk^2 - |a|^2 \mp \sqrt{|a|^4 - 1}| + |a|^2 + \sqrt{|a|^4 - 1} \\ &= ||a|^2 - \zeta| + |a|^2 + \sqrt{|a|^4 - 1} \\ &\leq \sqrt{f^2 - 1} + f^2 + \sqrt{f^4 - 1}. \end{aligned}$$

From this inequality we directly conclude $2k \leq \hat{k}(f)$.

In Theorem 5: Let $\zeta \in \mathbb{R}$. Arguing as above we find that every bifurcation point $(a, \zeta) \in \bar{\Gamma}_f$ satisfies equation (1.5) for some $k \in \mathbb{N}, \sigma \in \{-1, 1\}$ and hence gives rise to at most four bifurcation points. Therefore, in case $d < 0$, we have to prove $4k \leq \bar{k}(\zeta)$. Indeed, in that case the inequality $\zeta + dk^2 \geq \sqrt{3}$ from (1.5) implies $k \leq (|d|^{-1}(\zeta - \sqrt{3})_+)^{1/2}$ which is all we had to show.

4.4. Simplicity of the kernels.

In Theorem 4: Let $f \in \mathbb{R}$ and let $(\hat{a}(t), \hat{\zeta}(t))$ be a possible bifurcation point with respect to $\hat{\Gamma}_f$, i.e., we assume that $t \in (-1, 1)$ satisfies equation (1.4) for some $k \in \mathbb{N}$ and some $\sigma \in \{-1, 1\}$. Then Proposition 11 implies that $\ker(\hat{F}_a(0, t))$ is one-dimensional if and only if we have

$$(4.11) \quad -k^2 + d^{-1}(4|\hat{a}(t)|^2 - 2\hat{\zeta}(t)) \notin (\mathbb{N}_0 \setminus \{k\})^2.$$

Since we know from Lemma 6(a) that

$$4|\hat{a}(t)|^2 - 2\hat{\zeta}(t) = 2f^2(1 - t^2) - 2t(1 - t^2)^{-1/2}$$

(4.11) is guaranteed by condition (S) of Theorem 4 (iii) and we are done.

In Theorem 5: Let $\zeta \in \mathbb{R}$ and let $(\bar{a}(s), \bar{f}(s))$ be a possible bifurcation point with respect to $\bar{\Gamma}_\zeta$, i.e., we assume that s is given by (1.5) for some $k \in \mathbb{N}, \sigma \in \{-1, 1\}$. As above, Lemma 6(b) implies the equation

$$4|\bar{a}(s)|^2 - 2\zeta = 4s^2 - 2\zeta \stackrel{(1.5)}{=} \frac{2}{3} \left(\zeta + 4dk^2 - 2\sigma \sqrt{(\zeta + dk^2)^2 - 3} \right)$$

which shows that condition (S) from Theorem 5 (iii) guarantees the simplicity of $\ker(\bar{F}_a(0, s))$.

4.5. Transversality condition.

In the calculations related to the verification of the transversality condition we will use the following short-hand notations. In the context of Theorem 4 where (t, k) is a solution of (1.4) we write

$$a = (\hat{a}_1(t), \hat{a}_2(t)), \quad \zeta = \hat{\zeta}(t), \quad \dot{a} = \left(\frac{d\hat{a}_1}{dt}(t), \frac{d\hat{a}_2}{dt}(t) \right), \quad \dot{\zeta} = \frac{d\hat{\zeta}}{dt}(t)$$

and in the context of Theorem 5 where (s, k) is a solution of (1.5) we write

$$a = (\bar{a}_1(s), \bar{a}_2(s)), \quad f = \bar{f}(s), \quad \dot{a} = \left(\frac{d\bar{a}_1}{ds}(s), \frac{d\bar{a}_2}{ds}(s) \right), \quad \dot{f} = \frac{d\bar{f}}{ds}(s).$$

Furthermore we will use

$$\varphi(x) := \varphi_k(a)(x) = \alpha \cos(kx), \quad \varphi^*(x) := \varphi_k^*(a)(x) = \beta \cos(kx),$$

where the vectors $\alpha = \alpha^k, \beta = \beta^k \in \mathbb{R}^2$ were defined in (4.7), (4.8). We have to check the transversality condition in the possible bifurcation points that we determined in Section 4.2. Hence we may use (4.6), i.e.,

$$(\zeta + dk^2)^2 - 4(\zeta + dk^2)|a|^2 + 1 + 3|a|^4 = 0.$$

In view of the formulas (4.7) and (4.8) we will have to investigate the following cases:

- Case (1):* $|a_1 a_2| \neq \frac{1}{2}$ or $3a_1^2 + a_2^2 \neq \zeta + dk^2$
- Case (2):* $a_1 a_2 = \frac{1}{2}$ and $3a_1^2 + a_2^2 = \zeta + dk^2$
- Case (3):* $a_1 a_2 = -\frac{1}{2}$ and $3a_1^2 + a_2^2 = \zeta + dk^2$

In all three cases Proposition 9 yields the following formula for every constant $\psi \in \mathbb{R}^2 \subset H$:

$$\begin{aligned}
T(\psi) &:= \langle G_{aa}(a, \zeta, f)[\varphi, \psi], \varphi^* \rangle_H = \langle DG_{aa}(a, \zeta, f)[\varphi, \psi], \varphi^* \rangle_{L^2} \\
&= - \left\langle \begin{pmatrix} \varphi^T M_1(a) \psi \\ \varphi^T M_2(a) \psi \end{pmatrix}, \varphi^* \right\rangle_{L^2} \\
&\stackrel{(4.7)}{=} - \left\langle \begin{pmatrix} \alpha^T M_1(a) \psi \\ \alpha^T M_2(a) \psi \end{pmatrix} \cos(k \cdot), \beta \cos(k \cdot) \right\rangle_{L^2} \\
&= - \begin{pmatrix} \alpha^T M_1(a) \psi \\ \alpha^T M_2(a) \psi \end{pmatrix}^T \beta \int_0^\pi \cos(kx)^2 dx \\
&= - \pi \alpha^T \begin{pmatrix} 3a_1\beta_1 + a_2\beta_2 & a_1\beta_2 + a_2\beta_1 \\ a_1\beta_2 + a_2\beta_1 & a_1\beta_1 + 3a_2\beta_2 \end{pmatrix} \psi
\end{aligned}$$

Using (4.7), (4.8) and $(\zeta + dk^2)^2 - 4|a|^2(\zeta + dk^2) + 1 + 3|a|^4 = 0$ we find in case (1)

$$\begin{aligned}
&T(\psi) \\
&= -\pi \begin{pmatrix} a_1(-3 + 6a_1^2a_2^2 - 3a_2^4 + 9a_1^4 + (2a_2^2 - 6a_1^2)(\zeta + dk^2) + (\zeta + dk^2)^2) \\ a_2(-1 + 15a_1^4 + 3a_2^4 + 18a_1^2a_2^2 - (14a_1^2 + 6a_2^2)(\zeta + dk^2) + 3(\zeta + dk^2)^2) \end{pmatrix}^T \psi \\
&= -\pi \begin{pmatrix} a_1(-4 + 6a_1^4 - 6a_2^4 + (6a_2^2 - 2a_1^2)(\zeta + dk^2)) \\ a_2(-4 + 6a_1^4 - 6a_2^4 + (6a_2^2 - 2a_1^2)(\zeta + dk^2)) \end{pmatrix}^T \psi \\
&= -2\pi(-2 + 3a_1^4 - 3a_2^4 + (3a_2^2 - a_1^2)(\zeta + dk^2))a^T \psi.
\end{aligned}$$

In case (2) one has $\alpha = (2(a_2^2 - a_1^2), -2)^T$, $\beta = (-2, 0)^T$ and using $a_1a_2 = \frac{1}{2}$ one obtains

$$T(\psi) = 2\pi \alpha^T \begin{pmatrix} 3a_1 & a_2 \\ a_2 & a_1 \end{pmatrix} \psi = 2\pi \begin{pmatrix} 2a_1(3a_2^2 - 3a_1^2 - \frac{a_2}{a_1}) \\ 2a_2(a_2^2 - a_1^2 - \frac{a_1}{a_2}) \end{pmatrix}^T \psi = -2\pi(6a_1^2 - 2a_2^2)a^T \psi$$

while in case (3) we may use $\alpha = (2, 0)^T$, $\beta = (2(a_2^2 - a_1^2), 2)^T$ and $a_1a_2 = -\frac{1}{2}$ to get

$$T(\psi) = -2\pi \begin{pmatrix} 3a_1\beta_1 + a_2\beta_2 \\ a_1\beta_2 + a_2\beta_1 \end{pmatrix} \psi = -2\pi(2a_2^2 - 6a_1^2)a^T \psi.$$

Summarizing these calculations we find

$$(4.12) \quad T(\psi) = -2\pi a^T \psi \cdot \begin{cases} -2 + 3a_1^4 - 3a_2^4 + (3a_2^2 - a_1^2)(\zeta + dk^2) & \text{in case (1),} \\ 6a_1^2 - 2a_2^2 & \text{in case (2),} \\ 2a_2^2 - 6a_1^2 & \text{in case (3).} \end{cases}$$

In a similar way we obtain in case (1)

$$\begin{aligned}
\langle \varphi, \varphi^* \rangle_{L^2} &= \alpha^T \beta \int_0^\pi \cos(kx)^2 dx \\
&= \frac{\pi}{2} (-1 + 4a_1^2a_2^2 + (3a_1^2 + a_2^2 - \zeta - dk^2)^2) \\
&= \frac{\pi}{2} \left((\zeta + dk^2)^2 - 2(\zeta + dk^2)(3a_1^2 + a_2^2) - 1 + 4a_1^2a_2^2 + (3a_1^2 + a_2^2)^2 \right).
\end{aligned}$$

Using again $(\zeta + dk^2)^2 - 4|a|^2(\zeta + dk^2) + 1 + 3|a|^4 = 0$ in case (1) and performing the corresponding calculations for the cases (2) and (3) we arrive at

$$(4.13) \quad \langle \varphi, \varphi^* \rangle_{L^2} = \pi \begin{cases} (\zeta + dk^2)(-a_1^2 + a_2^2) - 1 + 3a_1^4 + 2a_1^2 a_2^2 - a_2^4 & \text{in case (1),} \\ 2a_1^2 - 2a_2^2 & \text{in case (2),} \\ 2a_2^2 - 2a_1^2 & \text{in case (3).} \end{cases}$$

Now we are going to use the formulas (4.12),(4.13) in the concrete settings of Theorem 4 and Theorem 5.

In Theorem 4: Let $f \in \mathbb{R}$ and let $t \in (-1, 1)$ satisfy equation (1.4) for some $k \in \mathbb{N}$ and some $\sigma \in \{-1, 1\}$. Since $\dot{a} \in \mathbb{R}^2 \subset H$ is a constant vector the formulas (4.12),(4.13) and Proposition 9 yield in case (1)

$$\begin{aligned} & \langle \hat{F}_{at}(0, t)[\varphi], \varphi^* \rangle_H \\ & \stackrel{(4.3)}{=} \langle G_{aa}(a, \zeta, f)[\varphi, \dot{a}], \varphi^* \rangle_H + \dot{\zeta} \langle G_{a\zeta}(a, \zeta, f)[\varphi], \varphi^* \rangle_H \\ & \stackrel{(4.12)}{=} -2\pi a^T \dot{a} (-2 + 3a_1^4 - 3a_2^4 + (3a_2^2 - a_1^2)(\zeta + dk^2)) + \dot{\zeta} \langle D^{-1}\varphi, \varphi^* \rangle_H \\ & = -2\pi a^T \dot{a} (-2 + 3a_1^4 - 3a_2^4 + (3a_2^2 - a_1^2)(\zeta + dk^2)) + \dot{\zeta} \langle \varphi, \varphi^* \rangle_{L^2} \\ & \stackrel{(4.13)}{=} \pi \left(-(-4 + 6a_1^4 - 6a_2^4 + (6a_2^2 - 2a_1^2)(\zeta + dk^2))a^T \dot{a} \right. \\ & \quad \left. + \dot{\zeta} ((\zeta + dk^2)(-a_1^2 + a_2^2) - 1 + 3a_1^4 + 2a_1^2 a_2^2 - a_2^4) \right). \end{aligned}$$

We will now insert the trivial solution $(a_1, a_2, \zeta) = (\hat{a}_1(t), \hat{a}_2(t), \hat{\zeta}(t))$ from Lemma 6 and use the identities

$$a^T \dot{a} = \frac{d}{dt} \frac{|\hat{a}(t)|^2}{2} = \frac{d}{dt} \frac{f^2(1-t^2)}{2} = -f^2 t, \quad \dot{\zeta} = -2f^2 t + (1-t^2)^{-3/2}.$$

Notice also that the necessary condition (4.6) for bifurcation becomes

$$\zeta + dk^2 = 2f^2(1-t^2) - \sigma \sqrt{f^4(1-t^2)^2 - 1}$$

so that (1.4) is proved. After a lengthy computation we obtain

$$\begin{aligned} & \langle \hat{F}_{at}(0, t)[\varphi], \varphi^* \rangle_H \\ & = \pi \left(4f^6 t^3 (1-t^2)^2 + f^4 (1-t^2)^{1/2} - 2t f^2 - (1-t^2)^{-3/2} \right. \\ & \quad \left. - \sigma \sqrt{f^4(1-t^2)^2 - 1} \left(4f^4 t^3 (1-t^2) + f^2 (2t^2 - 1)(1-t^2)^{-1/2} \right) \right) \end{aligned}$$

and hence the transversality condition (H2) from Theorem 8 is satisfied whenever the right-hand side is nonzero, i.e. when condition (T) holds. In case (2) or (3) the transversality condition is always satisfied. Indeed, proceeding as above and using the explicit formulas

$$a_1^2 = \frac{\sqrt{1-t^2}}{2|t|}, \quad a_2^2 = \frac{|t|}{2\sqrt{1-t^2}}, \quad f^2 = \frac{1}{2|t|(1-t^2)^{3/2}}$$

from Lemma 6 (a) we find in case (2), where $t < 0$, that

$$\begin{aligned}
\langle \hat{F}_{at}(0, t)[\varphi], \varphi^* \rangle_H &= T(\dot{a}) + \dot{\zeta} \langle \varphi, \varphi^* \rangle_{L^2} \\
&\stackrel{(4.12)}{=} -2\pi a^T \dot{a} (6a_1^2 - 2a_2^2) + \dot{\zeta} \cdot \pi (2a_1^2 - 2a_2^2) \\
&= 2\pi (f^2 t (6a_1^2 - 2a_2^2) + (-2f^2 t + (1 - t^2)^{-3/2})(a_1^2 - a_2^2)) \\
&= 2\pi (f^2 t \cdot 4a_1^2 + (1 - t^2)^{-3/2}(a_1^2 - a_2^2)) \\
&= -\frac{\pi}{|t|(1 - t^2)^2} \neq 0
\end{aligned}$$

and similarly in case (3), where $t > 0$, that

$$\langle \hat{F}_{at}(0, t)[\varphi], \varphi^* \rangle_H = +\frac{\pi}{|t|(1 - t^2)^2} \neq 0.$$

In Theorem 5: Now let $\zeta \in \mathbb{R}$ and let s be given by (1.5). Since $\dot{a} \in \mathbb{R}^2 \subset H$ is a constant vector we get from (4.12) and Proposition 9 in case (1)

$$\begin{aligned}
\langle \bar{F}_{as}(0, s)[\varphi], \varphi^* \rangle_H &\stackrel{(4.3)}{=} \langle G_{aa}(a, \zeta, f)[\varphi, \dot{a}], \varphi^* \rangle_H + \underbrace{\dot{f} \langle G_{af}(a, \zeta, f)[\varphi], \varphi^* \rangle_H}_{=0} \\
&\stackrel{(4.12)}{=} -2\pi a^T \dot{a} (-2 + 3a_1^4 - 3a_2^4 + (3a_2^2 - a_1^2)(\zeta + dk^2)).
\end{aligned}$$

Recalling

$$a^T \dot{a} = \frac{d}{ds} \frac{|\bar{a}(s)|^2}{2} = \frac{d}{ds} \frac{s^2}{2} = s$$

we obtain

$$\langle \bar{F}_{as}(0, s)[\varphi], \varphi^* \rangle_H = -2\pi s (-2 + 3a_1^4 - 3a_2^4 + (3a_2^2 - a_1^2)(\zeta + dk^2)).$$

Now we substitute $(a_1, a_2) = (\bar{a}_1(s), \bar{a}_2(s))$ from Lemma 6 and the value s from (1.5) of Theorem 5 to obtain after a lengthy calculation

$$\begin{aligned}
&\langle \bar{F}_{as}(0, s)[\varphi], \varphi^* \rangle_H \\
&= \frac{2\pi\sigma s}{27(1 + (s^2 - \zeta)^2)} \sqrt{(\zeta + dk^2)^2 - 3} \left(2\zeta + 5dk^2 - 4\sigma \sqrt{(\zeta + dk^2)^2 - 3} \right) \\
&\quad \cdot \underbrace{\left(4\zeta + dk^2 - 2\sigma \sqrt{(\zeta + dk^2)^2 - 3} \right) \left(\zeta + dk^2 + \sigma \sqrt{(\zeta + dk^2)^2 - 3} \right)}_{\neq 0}.
\end{aligned}$$

Hence, using $s \neq 0$ (from (4.6) we get $|s| = |a(s)| = |a| \geq 1$) we find that the transversality condition holds if and only if

$$\begin{aligned}
\zeta + dk^2 &\neq \sqrt{3} \quad \text{and} \quad 4\zeta + dk^2 - 2\sigma \sqrt{(\zeta + dk^2)^2 - 3} \neq 0 \\
&\quad \text{and} \quad 2\zeta + 5dk^2 - 4\sigma \sqrt{(\zeta + dk^2)^2 - 3} \neq 0
\end{aligned}$$

which is precisely assumption (T) in Theorem 5.

In case (2) and (3) we have $|T(\dot{a})| = 2\pi|s||3a_1^2 - a_2^2|$. So let us identify those values of a_1, a_2, s, ζ, d and $k \in \mathbb{N}_0$ where

$$a_1^2 a_2^2 = \frac{1}{4}, \quad 3a_1^2 = a_2^2 \text{ and } 3a_1^2 + a_2^2 = \zeta + dk^2 \geq \sqrt{3},$$

i.e., the situations in case (2), (3) where transversality fails. Since in this case $a_1^2 = 1/\sqrt{12}$, $a_2^2 = 3/\sqrt{12}$ we see that $s^2 = a_1^2 + a_2^2 = 2/\sqrt{3}$, i.e.,

$$s = \pm \sqrt{\frac{2}{\sqrt{3}}} \text{ and either } \zeta = -\frac{1}{\sqrt{3}} \text{ or } \zeta = \frac{5}{\sqrt{3}}.$$

In all of these cases $3a_1^2 + a_2^2 = \sqrt{3}$, i.e. d and k must be such that $\zeta^2 + dk^2 = \sqrt{3}$ so that the necessary conditions of bifurcation is satisfied but transversality fails. However, this is already covered by condition (T) which excludes $\zeta + dk^2 = \sqrt{3}$. This finishes part (iii) of Theorem 5.

5. ILLUSTRATIONS

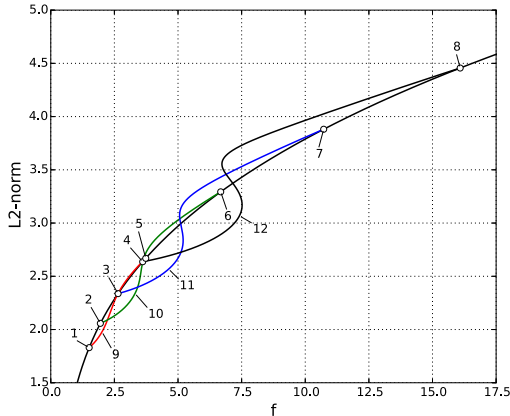
Below we highlight in five subsections different interesting features of our bifurcation results. All bifurcation diagrams are plotted with respect to the L^2 -norm of the solutions over the interval $(0, \pi)$. The L^2 -norm of a given solution represents the electrical power of the corresponding state inside the ring resonator. In order to illustrate our main results from Theorem 4 and Theorem 5 we numerically followed the primary bifurcation branches which emanate from the trivial curve. So-called points of secondary bifurcations, i.e., bifurcation points on these primary branches were very often detected by AUTO. However, for the sake of clarity, most of them were not included into our diagrams. In Sections 5.1 and 5.2 we illustrate the results of Theorem 5 for fixed ζ and for positive resp. negative dispersion coefficient d . In Sections 5.3 and 5.4 we show corresponding bifurcation diagrams based on Theorem 4. In Section 5.5 we demonstrate that dynamic detuning is a method to generate soliton combs as in [11].

5.1. The case $\zeta = 0, d = 0.1$. Here we have infinitely many bifurcation points on the trivial branch. Four pairs of those bifurcation points are shown. The trivial branch has no turning point and we only observe periodic Turing patterns. This means that the bifurcating solutions look as if they were multiples of the functions lying in the kernel of the linearized operator at the bifurcation point. In particular, no solitons were found.

The table provides some bifurcation points on the trivial branch. The bifurcation points at s given by (1.5) are predicted by Theorem 5 since the conditions (S) and (T) are satisfied. The f -values found by AUTO are listed as well.

k	σ	s	curve	f AUTO	f Thm 5	label
5	1	1.03235	red	1.50873	1.50871	1
5	-1	1.50582	red	3.73196	3.73195	5
6	1	1.16104	green	1.94874	1.94874	2
6	-1	1.85795	green	6.67731	6.67731	6
7	1	1.31863	blue	2.64489	2.64494	3
7	-1	2.18965	blue	10.72430	10.72430	7
8	1	1.48760	black	3.61248	3.61248	4
8	-1	2.51404	black	16.08740	16.08736	8

FIGURE 1. Bifurcation points on trivial branch.



Four bifurcating branches are depicted in the bifurcation diagram. All branches return to the trivial one. Their end points correspond to the same k . The labels 9-12 indicate solutions with k maxima ($k \in \{5, 6, 7, 8\}$) as shown below. They can be found on the branches emanating from bifurcation points associated to k via Theorem 5 (or Figure 1).

FIGURE 2. Bifurcation diagram

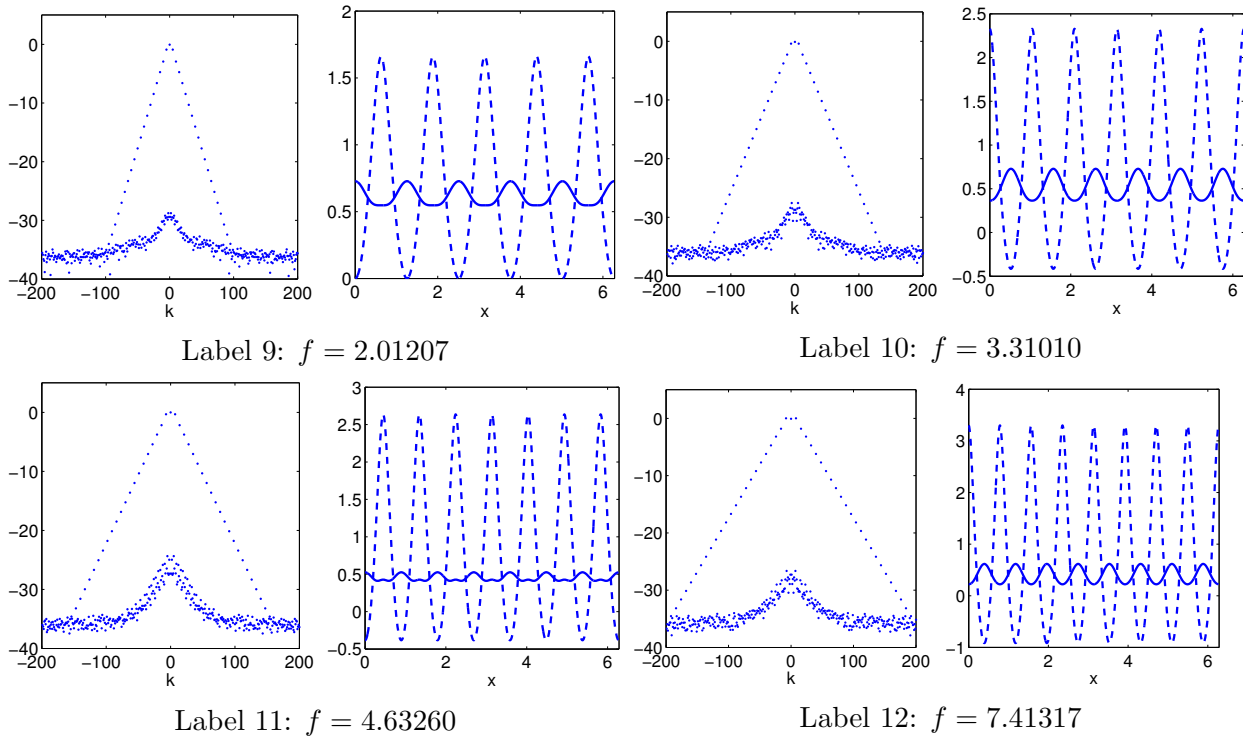


FIGURE 3. Selected solutions. Left: $\log(|\hat{a}(k)|)$; right: solid $a_1(x)$, dashed $a_2(x)$.

5.2. **The case $\zeta = 10, d = -0.2$.** In this example there are only finitely many (namely 12) bifurcation points on the trivial branch. The trivial branch has turning points and we find dark solitons. They occur in most pronounced form at the turning points of two nontrivial branches.

The table provides all bifurcation points on the trivial branch. The bifurcation points at s given by (1.5) are predicted by Theorem 5 since the conditions (S) and (T) are satisfied. The f -values found by AUTO are listed as well.

k	σ	s	curve	f AUTO	f Thm 5	label
1	1	1.82156	magenta	12.30707	12.30707	7
1	-1	3.12227	magenta	3.21945	3.21945	12
2	1	1.76678	brown	12.28057	12.28053	6
2	-1	3.02410	brown	3.97844	3.97844	11
3	1	1.67183	orange	12.16098	12.16097	5
3	-1	2.85277	orange	6.02862	6.02862	10
4	1	1.53017	blue	11.81841	11.81841	3
4	-1	2.59331	blue	8.87959	8.87959	9
5	1	1.33036	green	11.029645	11.02958	2
5	-1	2.21287	green	11.50750	11.50749	8
6	1	1.06458	red	9.499203	9.49913	1
6	-1	1.61245	red	12.04054	12.04060	4

FIGURE 4. Bifurcation points on trivial branch.

In the right diagram of Figure 5 one sees brown and magenta branches which bifurcate from the trivial curve at label 11 and 12 and connect to the blue and red branches at points of secondary bifurcation. Solitons were found at turning points, cf. labels 13 and 14. Their shapes are shown in Figure 6.

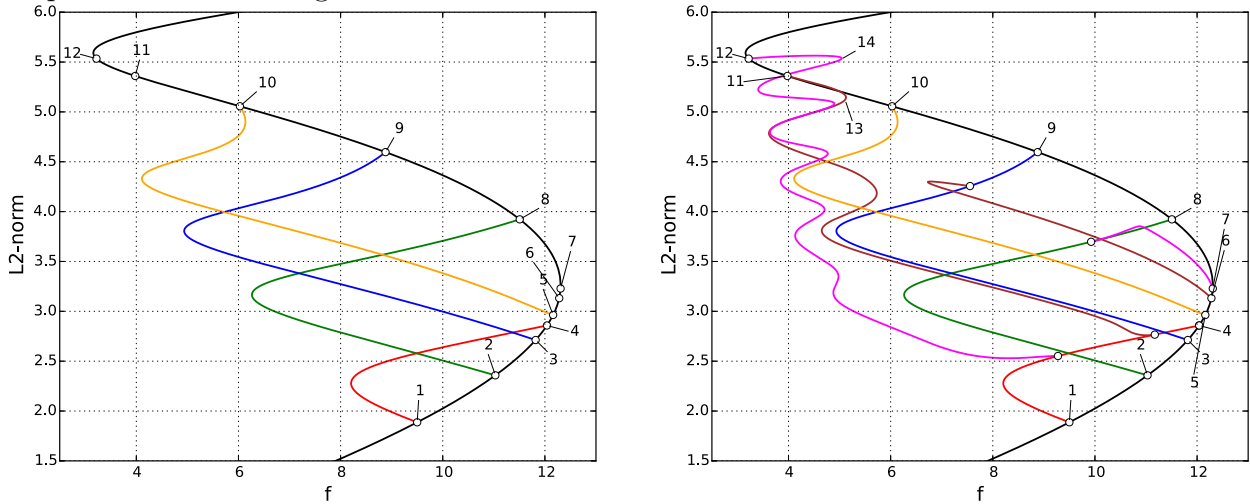
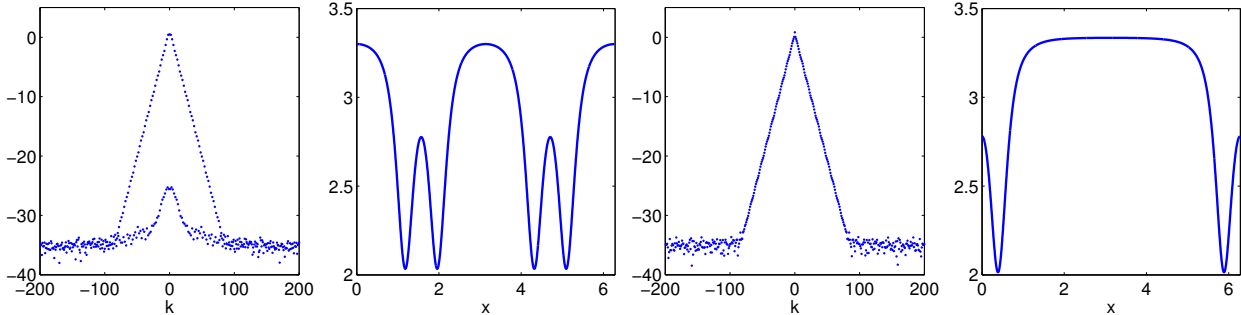


FIGURE 5. Bifurcation diagrams



Label 13: dark 4-soliton at $f = 5.10776$

Label 14: dark 2-soliton at $f = 5.02592$

FIGURE 6. Selected solutions. Left: $\log(|\hat{a}(k)|)$; right: $|a(x)|$.

5.3. **The case** $f = 1.6, d = 0.1$. This is an example with 14 bifurcation points on the trivial curve and many interesting features. Solitons are found at labels 15, 16, 17, 18 cf. Figures 10 and 11.

The table provides all bifurcation points on the trivial branch. The bifurcation points at $\zeta = \hat{\zeta}(t)$ are predicted by Theorem 4 since k, σ, t solve (1.4) and the conditions (S) and (T) are satisfied. The ζ -values found by AUTO are listed as well.

k	σ	t	curve	ζ AUTO	ζ Thm 4	label
1	1	0.10528	magenta	2.63750	2.63750	8
1	-1	0.77130	magenta	2.24888	2.24888	14
2	1	-0.18543	orange	2.28327	2.28327	6
2	-1	0.75556	orange	2.25196	2.25196	13
3	1	-0.52046	brown	1.25701	1.25702	4
3	-1	0.72127	brown	2.26952	2.26952	12
4	1	-0.72866	green	0.13681	0.13682	2
4	-1	0.66089	green	2.32248	2.32248	11
5	-1	-0.77281	red	-0.18665	-0.18666	1
5	-1	0.56321	red	2.42958	2.42954	10
6	-1	-0.61695	blue	0.80168	0.80166	3
6	-1	0.40312	blue	2.58451	2.58449	9
7	-1	-0.20600	pink	2.24085	2.24085	5
7	-1	0.01535	pink	2.57474	2.57475	7

FIGURE 7. Bifurcation points on trivial branch.

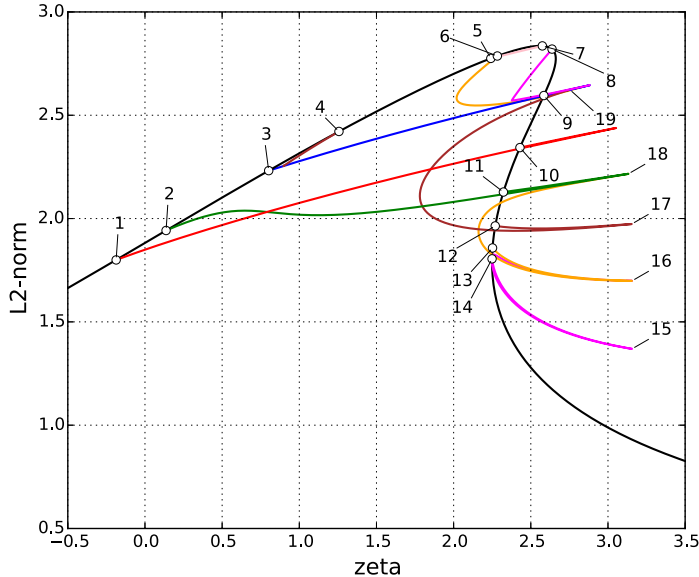


FIGURE 8. Bifurcation diagram

The brown branches, the magenta branch starting at label 8 and the orange branch starting at label 6 all enter the blue one. The orange branch going off label 12 enters the green one. A period-doubling bifurcation occurs when the brown branch going off label 4 meets the blue branch.

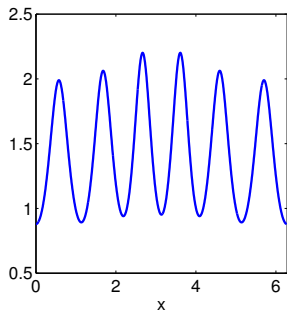


FIGURE 9. Label 19 at $\zeta = 2.75156$

At label 19 on the magenta branch we find a 2π -periodic solution with 6 maxima which is not $2\pi/6$ -periodic. In contrast, all solutions on the blue branch are $2\pi/6$ -periodic. The explanation is, that the $2\pi/6$ -periodicity is lost along the magenta branch which joins the blue one in a secondary bifurcation.

At the labels 15, 16, 17, 18 bright 1-, 2-, 3-, 4-solitons are found, respectively. They lie on branches emanating from bifurcation points associated to $k = 1, 2, 3, 4$, respectively.

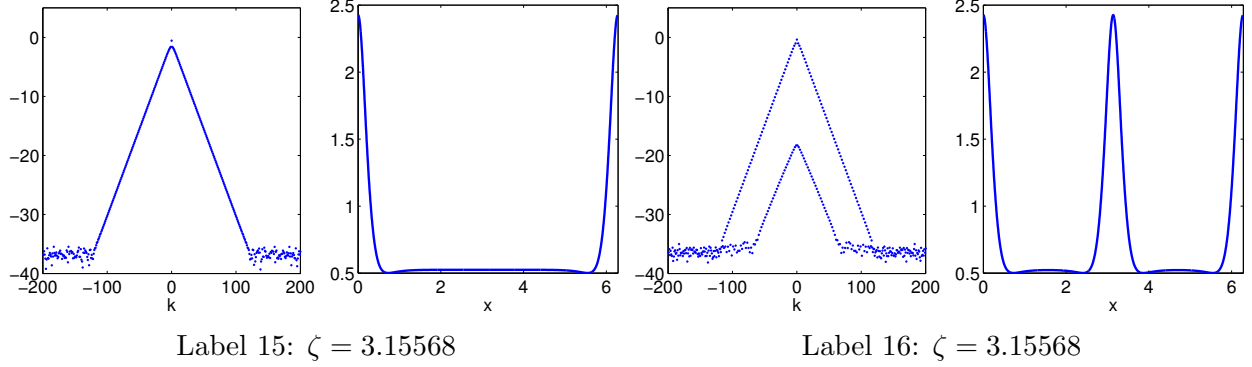


FIGURE 10. Selected solutions. Left: $\log(|\hat{a}(k)|)$; right: solid $|a(x)|$.

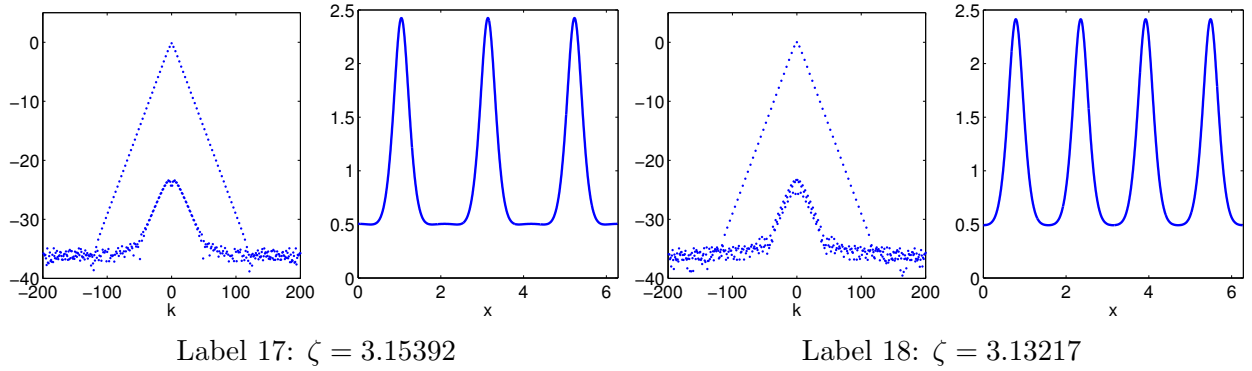


FIGURE 11. Selected solutions. Left: $\log(|\hat{a}(k)|)$; right: solid $|a(x)|$.

5.4. **The case $f = 2, d = -0.1$.** This is again an example with finitely many bifurcation points and dark solitons like in Section 5.2. Also here the dark solitons occur in most pronounced form at turning points of nontrivial branches.

The table provides all bifurcation points on the trivial branch. The bifurcation points at $\zeta = \hat{\zeta}(t)$ are predicted by Theorem 4 since k, σ, t solve (1.4) and the conditions (S) and (T) are satisfied. The ζ -values found by AUTO are listed as well.

k	σ	t	curve	ζ AUTO	ζ Thm 4	label
1	-1	0.85260	red	2.72386	2.72386	4
1	1	0.22806	red	4.02617	4.02619	1
2	-1	0.86118	blue	2.72771	2.72771	5
2	1	0.49553	blue	3.58829	3.58830	2
3	1	0.86262	green	2.72883	2.72883	6
3	1	0.78647	green	2.79924	2.79924	3

FIGURE 12. Bifurcation points on trivial branch.

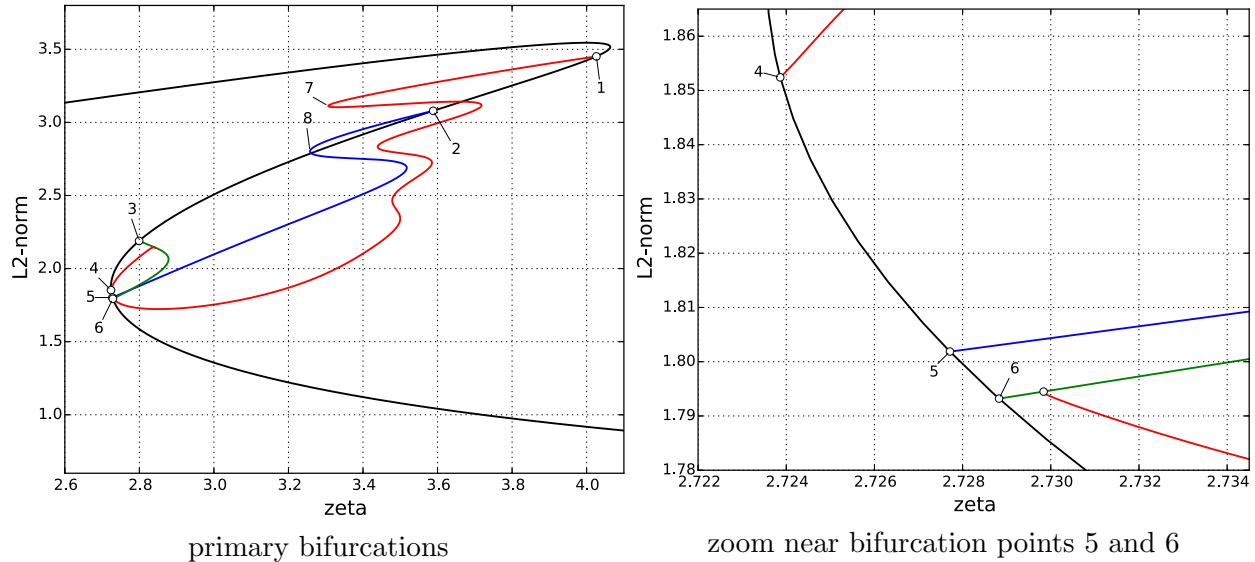
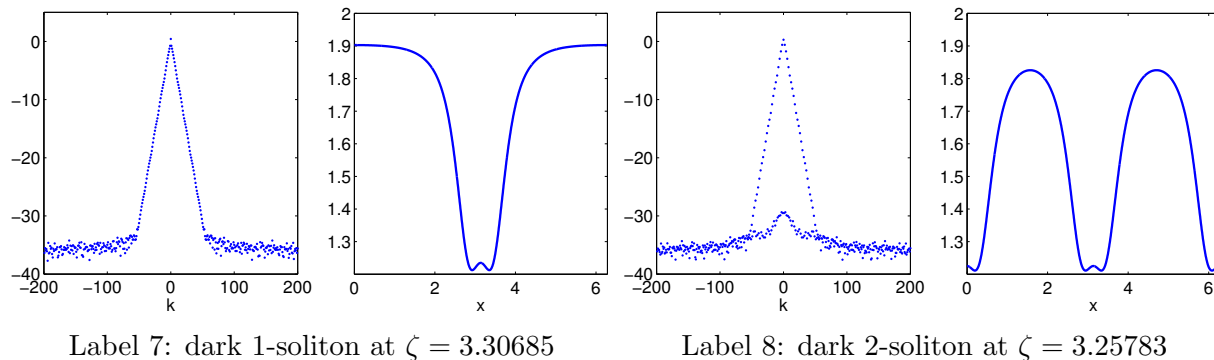


FIGURE 13. Bifurcation diagram

Both red branches ($k = 1$) enter the green one ($k = 3$) so that the trivial solutions at labels 1, 3, 4, 6 are connected to the dark 1-soliton at label 7 through nontrivial solutions. Similarly, the blue branch ($k = 2$) connects the trivial solutions at labels 2, 5 with the dark 2-soliton at label 8.

FIGURE 14. Selected solutions. Left: $\log(|\hat{a}(k)|)$; right: $|a(x)|$.

5.5. Time-dependent detuning and bifurcation diagrams. A typical problem in applications is the following: how can one drive the coupled laser/ring resonator into the 1-soliton state? A commonly used and quite practical idea is the use of time-dependent detuning [14]. Here the detuning $\zeta = \zeta(t)$ varies in time until it reaches its final value at which it stays, cf. Figure 15(a).

The mathematical model is given by the time-dependent Lugiato-Lefever equation

$$(5.1) \quad i\partial_t a(x, t) = (-i + \zeta(t))a(x, t) - d\partial_x^2 a(x, t) - |a(x, t)|^2 a(x, t) + if, \quad x \in (0, \pi), \quad t \in \mathbb{R}$$

with homogeneous Neumann boundary conditions at $x = 0$ and $x = \pi$. In our example we considered the low-power scenario of Section 5.3 with $f = 1.6$, $d = 0.1$ where 1-, 2- and 3-solitons exist for $\zeta = 2.67$, cf. Figure 8. A convenient choice for ζ is then given by the piecewise linear function

$$\zeta(t) = \begin{cases} -5 & 0 \leq t \leq T/30, \\ \frac{2.67+5}{T/3-T/30}(t - T/30) - 5 & T/30 \leq t \leq T/3, \\ 2.67 & T/3 \leq t \leq T \end{cases}$$

with $T = 1000$. With these choices we numerically integrated equation (5.1) starting from initial data given by the spatially constant steady-state solution at $\zeta = -5$ perturbed by a random function of size 10^{-14} . The numerical scheme is a Strang-splitting¹ in time as suggested in [13], and a pseudo-spectral method in space.

Depending on the (random) initial data we observe different scenarios for the evolution of the L^2 -norm. We show three of these scenarios in the following figures. The underlying picture is the bifurcation diagram (with respect to ζ) of the stationary equation from Figure 8. On top of this bifurcation diagram we plot in grey the time evolution of the L^2 -norm of the solution of (5.1).

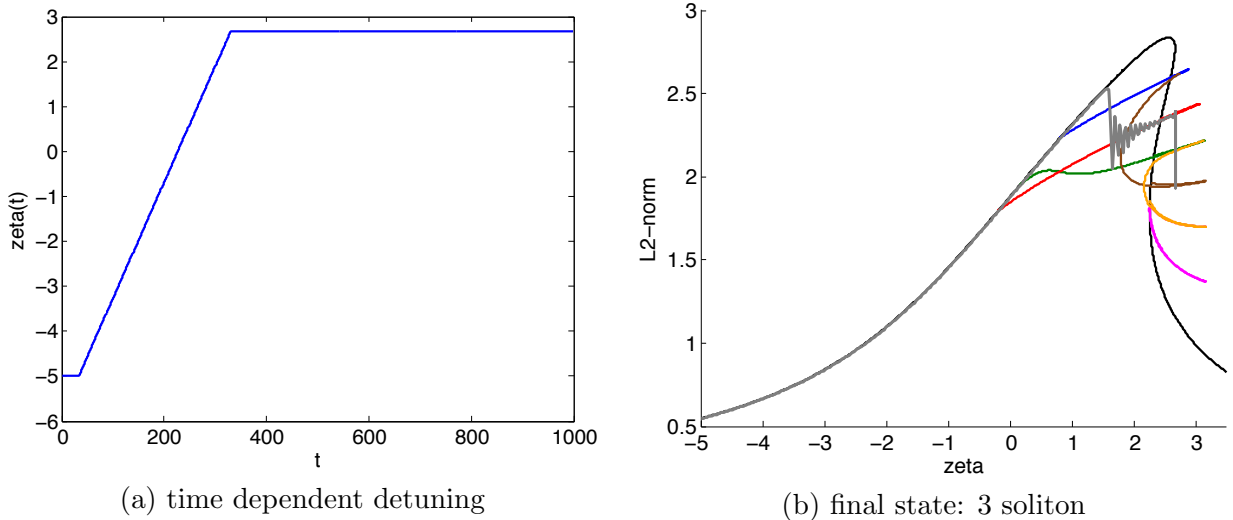


FIGURE 15. Time evolution of L^2 -norm in dynamic detuning

¹ In the Strang-splitting the linear inhomogeneous part (including the space derivatives and the forcing/damping terms) is propagated by an exponential integrator whereas the nonlinear part is solved exactly as for the standard NLS. It is proved in [13] that under certain regularity assumptions on the initial data (see Section 1.3) and the forcing/detuning the numerical method converges to the true solution of (5.1) on bounded time-intervals with order 2 in $L^2(0, \pi)$ and with order 1 in $H^1(0, \pi)$.

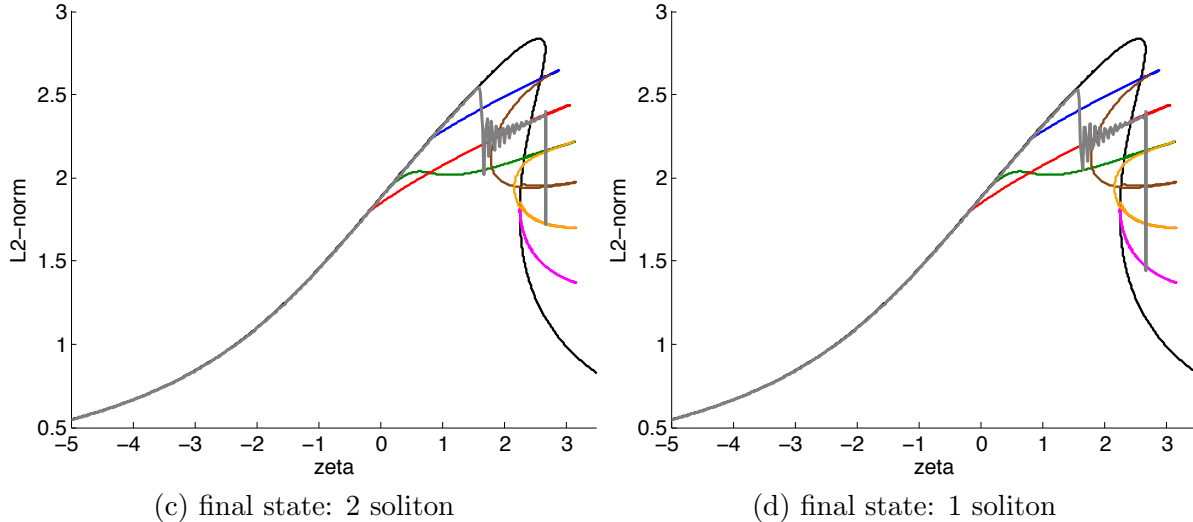


FIGURE 16. Time evolution of L^2 -norm in dynamic detuning

At the beginning of the time evolution the solution remains close to the constant one; the grey curve and the black curve practically overlap. When $\zeta(t)$ reaches a certain value between 1 and 2 the solution develops a spatially $\frac{2\pi}{5}$ -periodic pattern close to the red curve before passing to a k -soliton ($k \in \{1, 2, 3\}$) where the time evolution becomes numerically stationary. Qualitatively very similar time evolutions were observed by Herr et al. [11], p.148 for a different set of parameter values.² The strong similarity of time-dependent detuning simulations with our bifurcation diagrams suggests that the bifurcation diagrams may give important clues on the question how to drive the laser/ring resonator system into a soliton state. In particular, we conclude that the final soliton states of a time-dependent detuning approach typically lie on bifurcation curves that we have analytically characterized in Theorem 4 and Theorem 5.

6. CONCLUSIONS

Let us finally summarize our results from the point of view of their applicability. A first outcome of our analysis is that the search for frequency combs can from now on be reduced to specific parameter regimes. Theorem 1 shows for large $|f|$ and small $|d|$ that, roughly speaking, frequency combs satisfy the estimate $\|a\|_\infty = O(|f|^3|d|^{-1})$ uniformly with respect to ζ . In particular this result gives an upper bound for the maximal amplitude that one can expect for a highly localized soliton. In the case of normal dispersion $d < 0$ Theorem 2 shows that only trivial combs exist outside the explicit interval $[\zeta_*, \zeta^*]$ of detuning parameters. Here $\zeta_* < 0 < \zeta^*$, and $\zeta^*, -\zeta_* = O(f^6|d|^{-2})$ for large f and small $|d|$. A similar result holds for anomalous dispersion $d > 0$.

²As explained in the supplementary material to [11] the numerical integration method differs from ours since it is based on a time-dependent version of the coupled mode equations (1.6) instead of the Lugiato-Lefever equation (5.1).

Theorem 4 and 5 prove the existence of bifurcating branches of frequency combs and provide explicit formulae for the parameter values at which these branches emanate from the trivial ones. This is the analytical justification for what AUTO is successfully doing, i.e., finding bifurcation points and following bifurcation branches. The resulting bifurcation diagrams are quite complicated (cf. Section 5) and so far only few theoretical information about their structures has become apparent, see the remarks following Theorem 4. It remains open to investigate both analytically and numerically points of secondary bifurcation. The strong similarity of time-dependent detuning simulations with our bifurcation diagrams shows that the final soliton states of a laser/ring resonator system cannot be understood without the bifurcation phenomena that are the core of this paper.

The use of AUTO opens new possibilities to numerically compute the shape of specific frequency combs, and it allows to make observations and conjectures. Let us list two of them.

- We observed that in the bifurcation diagrams with respect to f the two solitons of Figure 6 appeared at turning points of the bifurcation curves, cf. Figure 5. The same happens in bifurcation diagrams with respect of ζ from Figure 8 and Figure 13. Also here the solutions with most pronounced soliton character, cf. Figures 10, 11, 14, lie on turning points of the branches. It will be worthwhile to investigate further if this observation is true in more general cases.
- Soliton combs are particularly important in applications and one would like to drive the pump-resonator system into such a state. Since all solitons were found on bifurcation curves connected to the trivial states time-dependent detuning seems to be a feasible way to eventually reach a soliton as outlined in Section 5.5.

We are aware that the last remark immediately leads to the important question about stability of solutions along branches. To the best of our knowledge AUTO does not offer a straightforward option that provides stability information for non-parabolic equations like (1.7). Locally near the bifurcation points the principle of exchange of stability (cf. [5, 15]) allows to analytically predict the stability or instability of solutions. Although this is an interesting piece of information, we refrained from elaborating it because of two reasons: it would have substantially enlarged the exposition and its validity is restricted only to small neighborhoods of the bifurcation points. Instead, it would be much more interesting to characterize the stability or instability globally along the branches. Analytically, this is very challenging and currently out of reach. It will be one of our future goals to attack this question numerically.

ACKNOWLEDGEMENTS

Both authors thank J. Gärtner, T. Jahnke, Ch. Koos, P. Palomo-Marin, J. Pfeifle, and Ph. Trocha (all from KIT) for fruitful discussions. We are grateful to T. Jahnke for letting us use two of his MATLAB codes: one that postprocesses AUTO data and generates

solution plots and one that performs the time integration of (5.1) via Strang-splitting. Additionally, both authors gratefully acknowledge financial support by the Deutsche Forschungsgemeinschaft (DFG) through the research grant MA 6290/2-1 (first author) and CRC 1173 (both authors).

REFERENCES

- [1] A.R. Bishop, M.G. Froest, D.W. McLaughlin, and E.A. Overman. A modal representation of chaotic attractors for the driven, damped pendulum chain. *Physical Letters A*, 144:17–25, 1990.
- [2] Y. K. Chembo and Nan Yu. Modal expansion approach to optical-frequency-comb generation with monolithic whispering-gallery-mode resonators. *Physical Review A*, 82:033801, 2010.
- [3] Stéphane Coen and Miro Erkintalo. Universal scaling laws of Kerr frequency combs. *Opt. Lett.*, 38(11):1790–1792, 2013.
- [4] Michael G. Crandall and Paul H. Rabinowitz. Bifurcation from simple eigenvalues. *J. Functional Analysis*, 8:321–340, 1971.
- [5] Michael G. Crandall and Paul H. Rabinowitz. Bifurcation, perturbation of simple eigenvalues and linearized stability. *Arch. Rational Mech. Anal.*, 52:161–180, 1973.
- [6] P. Del’Haye, A. Schliesser, O. Arcizet, T. Wilken, R. Holzwarth, and T.J. Kippenberg. Optical frequency comb generation from a monolithic microresonator. *Nature*, 450:1214–1217, 2007.
- [7] Miro Erkintalo and Stéphane Coen. Coherence properties of Kerr frequency combs. *Opt. Lett.*, 39(2):283–286, 2014.
- [8] C. Godey. A bifurcation analysis for the Lugiato-Lefever equation. *ArXiv e-prints*, July 2016.
- [9] Cyril Godey, Irina V. Balakireva, Aurélien Coillet, and Yanne K. Chembo. Stability analysis of the spatiotemporal Lugiato-Lefever model for Kerr optical frequency combs in the anomalous and normal dispersion regimes. *Phys. Rev. A*, 89:063814, 2014.
- [10] G. Haller. Homoclinic jumping in the perturbed nonlinear Schrödinger equation. *Comm. Pure Appl. Math.*, 52(1):1–47, 1999.
- [11] T. Herr, V. Brasch, J. Jost, C.Y. Wang, N.M. Kondratiev, M.L. Gorodetsky, and T.J. Kippenberg. Temporal solitons in optical microresonators. *Nature Photonics*, 8:145–152, 2014.
- [12] T. Herr, K. Hartinger, J. Riemensberger, C.Y. Wang, E. Gavartin, R. Holzwarth, M.L. Gorodetsky, and T.J. Kippenberg. Universal formation dynamics and noise of Kerr-frequency combs in microresonators. *Nature Photonics*, 6:480–487, 2012.
- [13] T. Jahnke, M. Mikl, and R. Schnaubelt. Strang splitting for a semilinear Schrödinger equation with damping and forcing. CRC 1173-Preprint 2016/4, Karlsruhe Institute of Technology, 2016.
- [14] Maxim Karpov, Hairun Guo, Erwan Lucas, Arne Kordts, Martin Pfeiffer, Victor Brasch, Grigory Lihachev, Valery Lobanov, Michael Gorodetsky, and Tobias Kippenberg. Universal dynamics and controlled switching of dissipative Kerr solitons in optical microresonators. In *Conference on Lasers and Electro-Optics*, page FM2A.2. Optical Society of America, 2016.
- [15] Hansjörg Kielhöfer. *Bifurcation theory*, volume 156 of *Applied Mathematical Sciences*. Springer, New York, second edition, 2012. An introduction with applications to partial differential equations.
- [16] T. J. Kippenberg, R. Holzwarth, and S. A. Diddams. Microresonator-based optical frequency combs. *Science*, 332:555–559, 2011.
- [17] Stefan Krömer, Timothy J. Healey, and Hansjörg Kielhöfer. Bifurcation with a two-dimensional kernel. *J. Differential Equations*, 220(1):234–258, 2006.
- [18] Ping Liu, Junping Shi, and Yuwen Wang. Bifurcation from a degenerate simple eigenvalue. *J. Funct. Anal.*, 264(10):2269–2299, 2013.
- [19] L. A. Lugiato and R. Lefever. Spatial dissipative structures in passive optical systems. *Phys. Rev. Lett.*, 58:2209–2211, 1987.
- [20] T. Miyaji, I. Ohnishi, and Y. Tsutsumi. Bifurcation analysis to the Lugiato-Lefever equation in one space dimension. *Phys. D*, 239(23-24):2066–2083, 2010.

- [21] Pedro Parra-Rivas, Damia Gomila, François Leo, Stéphane Coen, and Lendert Gelens. Third-order chromatic dispersion stabilizes Kerr frequency combs. *Opt. Lett.*, 39(10):2971–2974, 2014.
- [22] Paul H. Rabinowitz. Some global results for nonlinear eigenvalue problems. *J. Functional Analysis*, 7:487–513, 1971.
- [23] Shaofei Wang, Hairun Guo, Xuekun Bai, and Xianglong Zeng. Analysis of high-order dispersion on ultrabroadband microresonator-based frequency combs. *arXiv*, 1403.0183, 2014.
- [24] David Westreich. Bifurcation at double characteristic values. *J. London Math. Soc. (2)*, 15(2):345–350, 1977.

R. MANDEL

SCUOLA NORMALE SUPERIORE DI PISA,
I-56126 PISA, ITALY

Current address: Institute for Analysis, Karlsruhe Institute of Technology (KIT),
D-76128 Karlsruhe, Germany

E-mail address: Rainer.Mandel@kit.edu

W. REICHEL

INSTITUTE FOR ANALYSIS, KARLSRUHE INSTITUTE OF TECHNOLOGY (KIT),
D-76128 KARLSRUHE, GERMANY

E-mail address: wolfgang.reichel@kit.edu